

---

# Time to Corrosion of Reinforcing Steel in Concrete Containing Calcium Nitrite

---

PUBLICATION NO. FHWA-RD-99-145

OCTOBER 1999




U.S. Department of Transportation  
**Federal Highway Administration**

Research, Development, and Technology  
Turner-Fairbank Highway Research Center  
6300 Georgetown Pike  
McLean, VA 22101-2296



# FOREWORD

This report documents the findings of a 17-year study evaluating the long-term effectiveness of calcium nitrite as a corrosion inhibitor in chloride-contaminated reinforced concrete. A previous final report (FHWA-RD-88-165) discusses the data collected from 1980 to 1987. This report summarizes the work that was addressed in the previous report and presents the results of further tests and analyses. The report will be of interest to design firms and designers, bridge engineers, inspectors, construction contractors who are involved with reinforced concrete structures, and owners of such structures.



T. Paul Teng, P.E.  
Director, Office of Infrastructure  
Research and Development

# NOTICE

This document is disseminated under the sponsorship of the US Department of Transportation in the interest of information exchange. The United States Government or the State of Florida assumes no liability for its contents or use thereof. This report does not constitute a standard, specification, or regulation.

The United States Government or the State of Florida does not endorse products or manufacturers. Trade and manufacturers' names appear in this report only because they are considered essential to the object of the document.

### Technical Report Documentation Page

1. Report No. FHWA-RD-99-145	2. Government Accession No.	3. Recipient's Catalog No.	
4. Title and Subtitle TIME TO CORROSION OF REINFORCING STEEL IN CONCRETE CONTAINING CALCIUM NITRITE		5. Report Date October 1999	
		6. Performing Organization Code	
7. Author(s) R.G. Powers, A.A. Sagues, W.D. Cerlanek, C.A. Kasper, Lianfang Li		8. Performing Organization Report No.	
9. Performing Organization Name and Address Florida Department of Transportation 2006 NE Waldo Road Gainesville, Florida 32609		10. Work Unit No. 3D4G	
		11. Contract or Grant No. WPI No. 0510769	
12. Sponsoring Agency Name and Address Office of Infrastructure R&D Federal Highway Administration 6300 Georgetown Pike McLean, Virginia 22101-2296		13. Type of Report and Period Covered Final Report June 1996 to February 1998	
		14. Sponsoring Agency Code	
15. Supplementary Notes Contracting Officer's Technical Representative (COTR): Y.P. Virmani, HRDI Acknowledgments: Mario Paredes - FDOT, Andrew Donn - FDOT, Todd Hoyle - FDOT, Alicia Garcia-Rubio - USF			
16. Abstract In 1996, the Florida Department of Transportation received 18 slabs from the Federal Highway Administration. These slabs were cast in 1980 using predetermined amounts of calcium nitrite in chloride-contaminated reinforced concrete. These specimens were compared to reinforced slabs with no admixed calcium nitrite. The upper and lower steel mats were connected and remained connected until 1996. Various tests were conducted on these slabs until June 1987, after which all testing terminated and the slabs remained outdoors.  In 1996, the upper and lower reinforcing mats were disconnected. Prior to commencement of testing, the slabs were conditioned with water daily for two weeks. At the conclusion of all nondestructive testing, the slabs were autopsied to assess the condition of the reinforcing steel.  The findings of this study seem to indicate that calcium nitrite is effective in slowing the onset of corrosion in chloride-contaminated reinforced concrete as long as the ratio of chloride to nitrite does not exceed 0.9.			
17. Key Words Concrete, corrosion, reinforcing steel, macrocell current, corrosion inhibitor, calcium nitrite, rebars		18. Distribution Statement No restrictions. This document is available to the public through the National Information Service, Springfield, VA 22161.	
19. Security Classif. (of this report) Unclassified	20. Security Classif. (of this page) Unclassified	21. No. of Pages 46	22. Price

# SI\* (MODERN METRIC) CONVERSION FACTORS

## APPROXIMATE CONVERSIONS FROM SI UNITS

APPROXIMATE CONVERSIONS TO SI UNITS		APPROXIMATE CONVERSIONS FROM SI UNITS							
Symbol	When You Know	Multiply By	To Find	Symbol	When You Know	Multiply By	To Find	Symbol	
<b>LENGTH</b>				<b>LENGTH</b>					
in	inches	25.4	millimeters	mm	millimeters	0.039	inches	in	
ft	feet	0.305	meters	m	meters	3.28	feet	ft	
yd	yards	0.914	meters	m	meters	1.09	yards	yd	
mi	miles	1.61	kilometers	km	kilometers	0.621	miles	mi	
<b>AREA</b>				<b>AREA</b>					
in <sup>2</sup>	square inches	645.2	square millimeters	mm <sup>2</sup>	square millimeters	0.0016	square inches	in <sup>2</sup>	
ft <sup>2</sup>	square feet	0.093	square meters	m <sup>2</sup>	square meters	10.764	square feet	ft <sup>2</sup>	
yd <sup>2</sup>	square yards	0.836	square meters	m <sup>2</sup>	square meters	1.195	square yards	yd <sup>2</sup>	
ac	acres	0.405	hectares	ha	hectares	2.47	acres	ac	
mi <sup>2</sup>	square miles	2.59	square kilometers	km <sup>2</sup>	square kilometers	0.386	square miles	mi <sup>2</sup>	
<b>VOLUME</b>				<b>VOLUME</b>					
fl oz	fluid ounces	29.57	milliliters	mL	milliliters	0.034	fluid ounces	fl oz	
gal	gallons	3.785	liters	L	liters	0.264	gallons	gal	
ft <sup>3</sup>	cubic feet	0.028	cubic meters	m <sup>3</sup>	cubic meters	35.71	cubic feet	ft <sup>3</sup>	
yd <sup>3</sup>	cubic yards	0.765	cubic meters	m <sup>3</sup>	cubic meters	1.307	cubic yards	yd <sup>3</sup>	
NOTE: Volumes greater than 1000 l shall be shown in m <sup>3</sup> .									
<b>MASS</b>				<b>MASS</b>					
oz	ounces	28.35	grams	g	grams	0.035	ounces	oz	
lb	pounds	0.454	kilograms	kg	kilograms	2.202	pounds	lb	
T	short tons (2000 lb)	0.907	megagrams (or "metric ton")	Mg (or "t")	megagrams (or "metric ton")	1.103	short tons (2000 lb)	T	
<b>TEMPERATURE (exact)</b>				<b>TEMPERATURE (exact)</b>					
°F	Fahrenheit temperature	5(F-32)/9 or (F-32)/1.8	Celsius temperature	°C	Celsius temperature	1.8C + 32	Fahrenheit temperature	°F	
<b>ILLUMINATION</b>				<b>ILLUMINATION</b>					
fc	foot-candles	10.76	lux	lx	lux	0.0929	foot-candles	fc	
fl	foot-Lamberts	3.426	candela/m <sup>2</sup>	cd/m <sup>2</sup>	candela/m <sup>2</sup>	0.2919	foot-Lamberts	fl	
<b>FORCE and PRESSURE or STRESS</b>				<b>FORCE and PRESSURE or STRESS</b>					
lbf	poundforce	4.45	newtons	N	newtons	0.225	poundforce	lbf	
lbf/in <sup>2</sup>	poundforce per square inch	6.89	kilopascals	kPa	kilopascals	0.145	poundforce per square inch	lbf/in <sup>2</sup>	

\* SI is the symbol for the International System of Units. Appropriate rounding should be made to comply with Section 4 of ASTM E380.

(Revised September 1993)

# Table of Contents

INTRODUCTION .....	1
DESCRIPTION OF SPECIMENS .....	1
TESTING PROCEDURES .....	3
<i>Visual Survey</i> .....	3
<i>Intermat Resistance</i> .....	4
<i>Concrete Surface Resistivity</i> .....	4
<i>Half-Cell Potentials</i> .....	4
<i>Polarization Resistance</i> .....	5
<i>Electrochemical Impedance Spectroscopy</i> .....	5
<i>Macrocell Current</i> .....	5
<i>Carbonation Depth</i> .....	5
<i>Chloride Content and Profiling</i> .....	5
<i>Total and Free Nitrite Ion Profiling</i> .....	6
<i>Rebar Condition Assessment</i> .....	6
RESULTS AND INTERPRETATION .....	7
<i>Visual Assessment</i> .....	7
<i>Electrochemical Corrosion Assessment</i> .....	9
<i>Concrete Carbonation, Chloride, and Nitrite Analysis</i> .....	15
<i>Effect of Calcium Nitrite on Corrosion Performance</i> .....	20
CONCLUSIONS .....	24
REFERENCES .....	26
APPENDIX A. PHOTOGRAPHS SHOWING SPECIMEN AND TOP STEEL MAT CONDITIONS .....	28
APPENDIX B. ILLUSTRATION OF METHODS USED FOR REPORTING NITRITE CONTENT AND ANALYSIS RESULTS .....	37
<i>Admixed Nitrite</i> .....	37
<i>Total Nitrite</i> .....	37
<i>Free Nitrite</i> .....	37
REFERENCES .....	38

## List of Figures

<u>Figure</u>	<u>Page</u>
1: FHWA test specimens upon arrival at FDOT Materials Office . . . . .	2
2: Standard slab design . . . . .	3
3: Specimens with coring apparatus . . . . .	6
4: Arrangement used to determine free nitrites as a function of depth in slab cores . . . . .	7
5: Top mat of steel removed from all slabs for analysis . . . . .	7
6: Nominal macrocell current measured in 1997 as function of percentage of rebar area affected by corrosion. . . . .	12
7: 1980-1997 nominal macrocell current density as a function of top mat apparent corrosion current density from 1997 polarization resistance measurements . . . . .	13
8: Carbonation depth for all specimens . . . . .	15
9: History of chloride content at top rebar for all specimens . . . . .	15
10: Profiles of total chlorides incrementally measured through the thickness of seven specimens . . . . .	17
11: Profiles of total measured nitrites as a percentage of the originally admixed nitrites for eight specimens . . . . .	17
12: Comparison of nitrite analysis results obtained with the method used in this work and by an independent laboratory . . . . .	18
13: Profiles of free nitrites as measured in cavity water for six specimens . . . .	19

**List of Figures (Cont.)**

<u>Figure</u>	<u>Page</u>
14: Percentage of rebar surface area affected by corrosion as a function of top mat chloride content at the end of the ponding period . . . . .	21
15: Macrocell current density as a function of top mat chloride content at the end of the ponding period . . . . .	22
16: Percentage of rebar surface area affected by corrosion as a function of top mat 1997 nitrite content minus 1997 chloride content . . . . .	23
17: Macrocell current density as a function of top mat 1997 nitrite content minus 1997 chloride content . . . . .	24
Appendix A: Slabs 211-228, visual condition of all slabs in 1997 and top steel mats in 1998 . . . . .	28

## List of Tables

<u>Table</u>	<u>Page</u>
1: Properties of Fine and Coarse Aggregate Used in Test Specimens . . . . .	1
2: Concrete Mix Design . . . . .	2
3: Specimen Characteristics Matrix . . . . .	4
4: Visual Assessment of Concrete Surface Conditions and Top Reinforcement Mat Analysis . . . . .	8
5: Results from Non-Destructive Testing . . . . .	10
6: Reinforcement Mat Potentials Versus CSE and Computed Potential Differences Between Mats . . . . .	11
7: Macrocell Current and Theoretical Iron Consumed . . . . .	14
8: Results from Destructive Testing . . . . .	16



## INTRODUCTION

In 1980, the Federal Highway Administration (FHWA) began a 6 year research project to investigate the effects of calcium nitrite on salt-contaminated reinforced concrete. This project was prompted by the need to protect the Nation's bridges and structures from damage due to corrosion. Calcium nitrite is reported to chemically inhibit breakdown of the passivating layer of the embedded reinforcement.<sup>(1)</sup> The initial research focused on the long-term results of calcium nitrite in chloride-contaminated reinforced concrete, concluding that the use of calcium nitrite was effective in reducing the rate of corrosion when the nitrite content was greater than the chloride content at reinforcement depth.<sup>(2-3)</sup>

For the purposes of the earlier investigation, the slabs containing varying amounts of admixed chlorides were ponded in December 1980 for 46 days with a 3 percent sodium chloride solution. After which time, the ponds were removed, chloride concentrations in the concrete were determined at the rebar depth, and the specimens were exposed to natural weather conditions. Routine testing performed on the specimens included the measurement of macrocell current, driving voltage, half-cell potentials, and alternating current (AC) resistance. Testing for the project concluded in June 1987, with the final data collected 2,429 days after initial ponding. After which, the specimens remained exposed to natural weather conditions in the Washington, D.C. area. In 1996, the slabs were transported to the Florida Department of Transportation (FDOT) State Materials Office in Gainesville, where they were prepared for final electrochemical testing and specimen autopsy. FDOT testing was carried out 6,170 days after initial ponding. Information obtained from these final tests was utilized to evaluate long-term stability characteristics of calcium nitrite in reinforced concrete, as well as the corrosion-inhibiting effectiveness of calcium nitrite in reinforced concrete with varying chloride contents.

## DESCRIPTION OF SPECIMENS

In the original study,<sup>(2)</sup> 18 specimens were cast to evaluate the effects of calcium nitrite in chloride-contaminated reinforced concrete (figure 1). The specimens measured 61 cm x 152 cm x 15 cm (2 ft x 5 ft x 0.5 ft) and were cast in two lifts. All lower lifts were cast from chloride-free concrete. The upper lifts were cast 1 to 3 days after the lower lifts, and contained varying amounts of sodium chloride. Calcium nitrite ( $\text{Ca}(\text{NO}_2)_2$ ) was admixed into both lifts of select specimens in the amount of 2.75 percent of the cement weight. This corresponds to  $10.7 \text{ kg/m}^3$  ( $18.1 \text{ lb/yd}^3$ ) of calcium nitrite, or  $7.48 \text{ kg/m}^3$  ( $12.6 \text{ lb/yd}^3$ ) of nitrite ( $\text{NO}_2^-$ ). The mixing ratio for the concrete was 1 part cement to 1.76 parts fine aggregate to 2.36 parts coarse aggregate. Table 1 lists the physical characteristics of the fine and coarse aggregates used for these specimens.

Table 1  
Properties of Fine and Coarse Aggregates Used in Test Specimens

Material	Specific Gravity	Fineness Modulus	Maximum Size
White Marsh Sand	2.64	2.6	0.075 mm (0.003 in)
Riverton Limestone	2.77	N/A	19 mm (0.75 in)

The coarse aggregate was graded to the mid-point of the American Association of State Highway and Transportation Officials (AASHTO) M-43 size number 67 specification. All coarse aggregates were separated

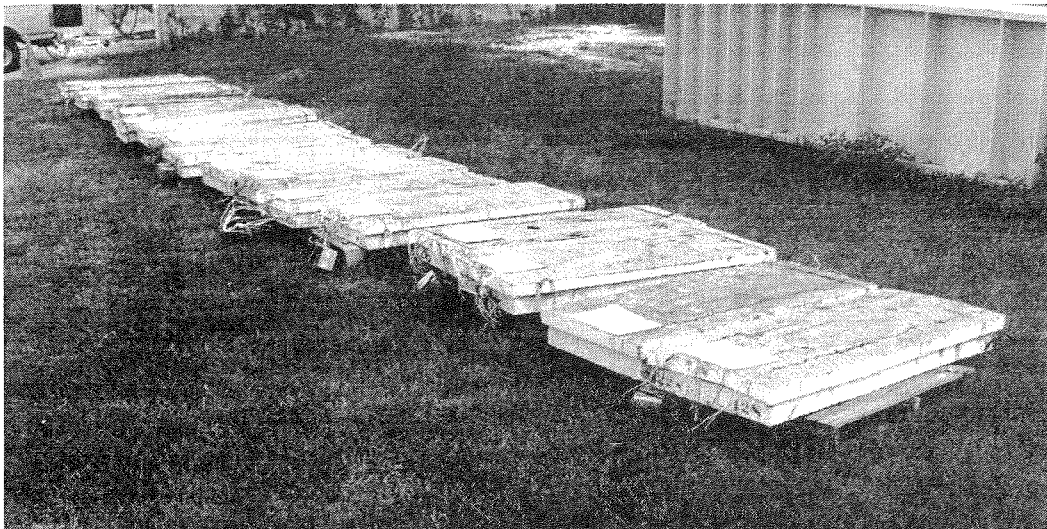


**Figure 1 - FHWA test specimens upon arrival at FDOT Materials Office.**

into four sizes which were then batched separately to ensure gradation control. The concrete was batched in a rotary drum mixer with a capacity of 0.31 m<sup>3</sup> (11 ft<sup>3</sup>). The size of each mix was 0.25 m<sup>3</sup> (9 ft<sup>3</sup>). The lower lift was covered with wet burlap during the curing period. This lift was wire brushed prior to placement of the upper lift. The upper lift was cured with wet burlap and polyethylene for 14 days.<sup>(2)</sup> Mix design properties are listed in table 2.

**Table 2  
Concrete Mix Design**

<b>Cement (7 Bags)</b>	390 kg/m <sup>3</sup> (658 lb/yd <sup>3</sup> )
<b>Water to Cement Ratio (w/c)</b>	0.53
<b>Fine Aggregate</b>	688 kg/m <sup>3</sup> (1160 lb/yd <sup>3</sup> )
<b>Coarse Aggregate</b>	920 kg/m <sup>3</sup> (1550 lb/yd <sup>3</sup> )
<b>Darex Air Entraining Agent</b>	379 mL/m <sup>3</sup> (9.81 oz/yd <sup>3</sup> )
<b>Unit Weight</b>	2215 kg/m <sup>3</sup> (138 lb/ft <sup>3</sup> )
<b>Air Content</b>	7% (±1.5%)
<b>Slump</b>	5 to 8 cm (2 to 3 in)

The upper lift of each specimen contained four longitudinal pieces of Number 5 rebar, 130 cm (51 in) long and two Number 4 transverse bars 46 cm (18 in) in length. All bars in the upper lift were tied together with steel wire. The lower mat consisted of seven pieces of Number 5 rebar, again 130 cm (51 in) long, and three Number 4 transverse bars 46 cm (18 in) long. All bars in the lower lift were welded. There was 1.9 cm (0.75 in) of cover above the upper mat, 2.5 cm (1 in) of cover below the lower mat, and 5 cm (2 in) of spacing between the upper and lower mats. The rebar used in these mats meets the specifications of AASHTO M-31. The standard configuration of the steel reinforcement for the slabs as well as typical slab dimensions are shown in figure 2. The connection between upper and lower steel mats no longer existed for most specimens upon arrival at the FDOT. All remaining specimen mats that were still connected were disconnected several weeks before testing and allowed to stabilize. Further specifics of the specimen design matrix are listed in table 3.

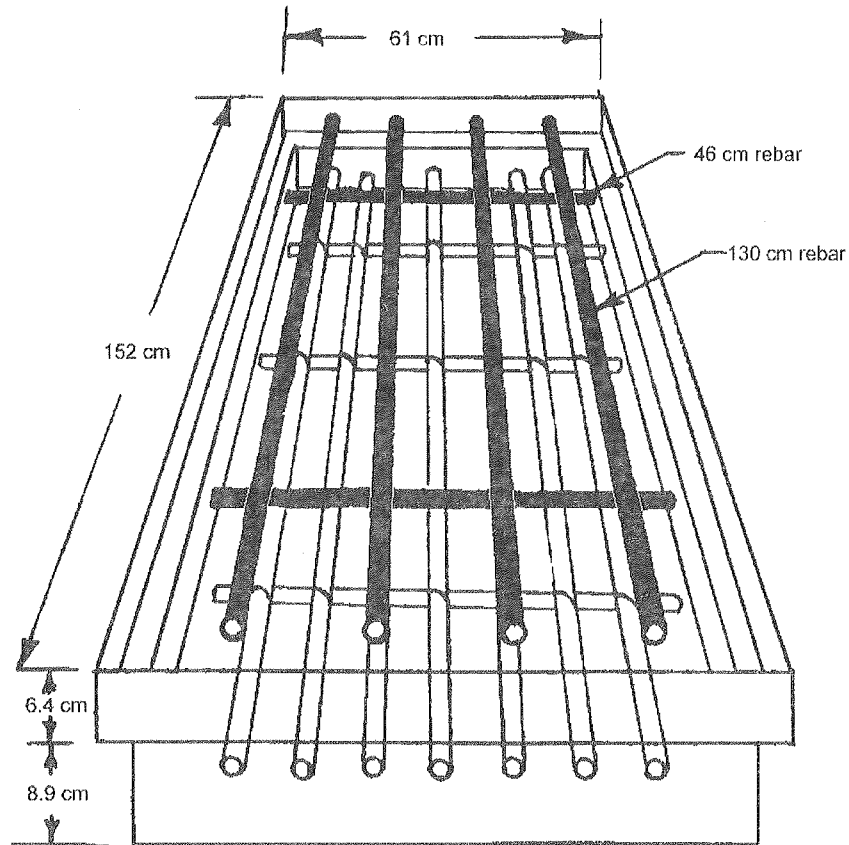


Figure 2 - Standard slab design.<sup>(2)</sup>

## TESTING PROCEDURES

All test slabs were moved to an indoor testing facility to eliminate the effects of direct sunlight and rain. The slabs were saturated with fresh water and covered for 14 days before testing commenced. Continuity between all top mat bars was established and maintained for a minimum of 48 hours before testing. All bottom mat bars were also connected and continuity was maintained for at least 48 hours. Upper and lower mats were left disconnected from each other and allowed to stabilize for a minimum of 24 hours. Non-destructive and destructive tests were then performed on each slab. All slabs continued to be saturated with water and covered overnight during the testing period.

The non-destructive testing and evaluation performed on each slab included: Visual survey, intermat resistance, concrete surface resistivity, half-cell potentials, polarization resistance ( $R_p$ ), electrochemical impedance spectroscopy (EIS), and macrocell current.

### *Visual Survey*

Each slab was inspected and photographed. Any exterior corrosion staining and cracking was recorded.

**Table 3**  
**Specimen Characteristics Matrix**

Slab	Unit Weight (kg/m <sup>3</sup> )	Percent Air	Ponded	7.48 kg/m <sup>3</sup> NO <sub>2</sub> in Both Lifts	Admixed CF into Top Lift (kg/m <sup>3</sup> )					
					3.0	5.9	8.9	12	15	21
211	2240	6.9	✓							
216	2260	6.0	✓	✓						
213	2240	6.4	✓		✓					
214	2240	6.4	✓		✓					
218	2270	6.8	✓	✓	✓					
219	2270	6.8	✓	✓	✓					
220	2270	7.0	✓	✓		✓				
221	2270	7.0	✓	✓		✓				
222	2290	6.0	✓	✓			✓			
223	2290	6.0	✓	✓			✓			
224	2340	7.5	✓	✓				✓		
225	2340	7.5	✓	✓				✓		
226	2350	7.3	✓	✓					✓	
227	2350	7.3	✓	✓					✓	
215	2310	5.5	✓							✓
228	—	5.5	✓	✓						✓
212	2320	6.9								
217	2260	6.0		✓						

***Intermat Resistance***

The AC resistance between the top and bottom mats of each slab was measured with a four-terminal 120-Hz AEMC Model 4500 Digital Ground Resistance Tester set up as a two-terminal device.

***Concrete Surface Resistivity***

A four-pin resistivity meter (CNS Electronics Model HM-247-2) was used to measure the concrete surface resistivity of each of the top slabs. The interprobe spacing was set at 5 cm (2 in). Measurements were taken longitudinally in the center of the slab, and longitudinally 15 cm (6 in) from center in both directions.

***Half-Cell Potentials***

Potentials between the top mat and a Cu/CuSO<sub>4</sub> reference electrode (CSE) were measured at 12 positions on the top face of each slab. The same 12 positions were again used to measure bottom mat CSE potentials.

### *Polarization Resistance*

Testing was performed with a Gamry CMS device on all slabs, with a CSE as reference placed on the center of the top of the slab, the top mat as the working electrode, and the bottom mat as the counter electrode. The tests began at the open circuit potential and produced a forward scan of 12 mV, followed by a reverse scan of 12 mV back to the open circuit potential. The scan rate was 0.1 mV/s. After a rest period, identical tests were run with the bottom mat as the working electrode and the top mat as the counter. Total resistance and solution resistance ( $R_s$ ) values were then derived by calculating tangent slopes of the resulting voltage vs. current plots.

### *Electrochemical Impedance Spectroscopy*

AC impedance testing using a Gamry CMS device was performed on all slabs with a CSE reference electrode: first with the top mat as the working electrode and the bottom mat as the counter electrode, then again with the bottom mat as the working electrode and the top mat as the counter electrode. The frequency range for each test varied from 1 mHz to 5 kHz. The initial potential was the open circuit potential and the amplitude for each test was 10 mV root mean square (rms). By presenting the test results on a Nyquist plot, solution resistance was estimated and compared to those values calculated from the polarization resistance testing. Once the values were verified, they were used in obtaining polarization resistance values by subtracting  $R_s$  from total resistance.

### *Macrocell Current*

After all other electrochemical tests were completed, a 10 minute polarization test was conducted to measure the capability of each slab to deliver a macrocell current between the top and bottom mats. A Hewlett Packard Model 34401A multimeter was then connected as a low-impedance ( $5 \Omega$ ) ammeter between both mats and current readings were recorded every second through a serial connection to a computer. The value of the current at 10 minutes was reported as the nominal macrocell current for the slab. The symbols  $I_{\text{macro}}$  and  $i_{\text{macro}}$  will be used to designate macrocell currents and current densities, respectively (nominal or otherwise), in figure axis labels.

Destructive testing performed on each slab included: Carbonation depth, chloride content and profiling, total and free nitrite ion profiling, and rebar condition assessment.

### *Carbonation Depth*

A sample was removed from each slab and immediately sprayed with phenolphthalein indicator to test concrete carbonation depth.

### *Chloride Content and Profiling*

Concrete cores were removed from each slab (figure 3). At the rebar depth in the top and bottom mats of each slab, chloride content was determined using an acid-soluble titration procedure in accordance with Florida Method FM 5-516.<sup>(4)</sup> These values were compared to those obtained in the previous study<sup>(2)</sup> to analyze each specimen's chloride redistribution. In addition, seven slabs (216, 219, 220, 223, 224, 226, and 228) had chloride contents evaluated at several depths to obtain total profiles.

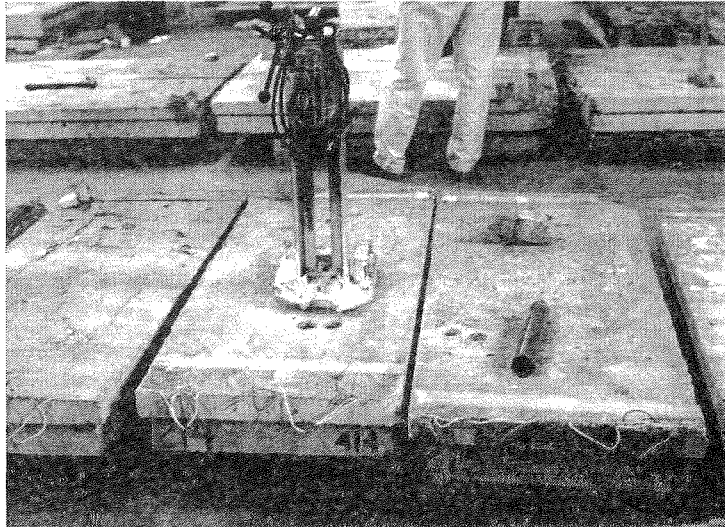


Figure 3 - Specimens with coring apparatus.

### *Total and Free Nitrite Ion Profiling*

Complete profiles for total and free nitrite concentrations were obtained on eight slabs (216, 217, 219, 220, 223, 224, 226, and 228). For the purposes of this report, total nitrite concentration is defined as the maximum amount that could be recovered by leaching the powdered concrete in water. Free nitrite concentration is defined here as the amount of nitrite present in the pore water of the concrete when the concrete has been allowed to stabilize in a 100 percent relative humidity environment. To determine total nitrite concentrations, concrete cores were sliced and then pulverized to pass a #50 sieve. Two grams of concrete powder were mixed with 1000 mL of distilled water for 24 hours and then the solution was filtered through Whatman #41 filter paper. The solution from this first extraction was analyzed for nitrite by spectrophotometric absorption at 543 nm.<sup>(5)</sup> The residue after the first extraction was further mixed with 500 mL of distilled water for an additional 10 days. The solution was then filtered again and measured for the residual nitrite. The sum of the amounts extracted in the first and second extractions was reported as the total nitrite, expressed first in wt % of the concrete and then converted in mass per unit volume using the concrete unit weight in table 2. To facilitate comparison, the results have been shown graphically as a percentage of the initially admixed nitrite. For evaluating free nitrites, water injected into small cavities was allowed to nearly equilibrate with concrete pore solution in the cores (which were kept in a 100% relative humidity chamber) as shown in figure 4, following a procedure described elsewhere.<sup>(5-6)</sup> Separate experiments have shown that the nitrite content of the water in the test cavities approaches that obtained by conventional pore water expression methods.<sup>(5)</sup> Free nitrites were then reported as the amount measured spectrophotometrically in the cavity water and expressed as g of  $\text{NO}_2^-$  per  $10^6$  g of water (parts per million or ppm). Calculation examples are provided in Appendix B.

### *Rebar Condition Assessment*

The top lift of each slab was demolished to retrieve the six-bar steel mats (figure 5). Percentage of surface area affected by corrosion and maximum pit depth were recorded for each bar.

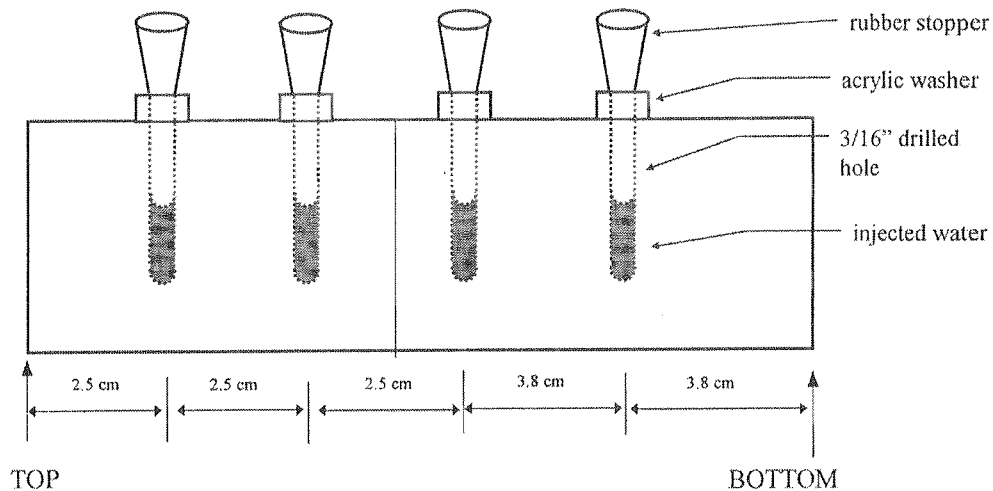


**Figure 4 - Arrangement used to determine free nitrites as a function of depth in slab cores (not to scale).**

## RESULTS AND INTERPRETATION

Since research performed for this project is a continuation of a previous FHWA investigation, selected results obtained are tabulated along with earlier results reported in FHWA Report No. FHWA-RD-88-165.<sup>(2)</sup> These data are included in tables 4, 5, 6, and 7.

### *Visual Assessment*

Visual slab inspection and steel reinforcement assessment data are summarized in table 4 for the 18 specimens. Photographs showing specimen and top steel mat conditions are in Appendix A. These samples were visually inspected, and in most instances, slab conditions were in close agreement with the visual assessment in 1987.



**Figure 5 - Top mat of steel removed from all slabs for analysis.**

**Table 4**  
**Visual Assessment of Concrete Surface Conditions and Top Reinforcement Mat Analysis**

SLAB NO.	YEAR OF TEST	VISUAL ASSESSMENT OF CONCRETE	VISUAL REBAR CORROSION ASSESSMENT	NUMBER OF BARS AFFECTED	MEASURED % S. AREA AFFECTED	MAX PIT DEPTH (cm)	CLASS*
211	1987	No cracking, no staining	†	†	†	†	†
	1997	No cracking, no staining	LIGHT	4	4.5	0.13	1
216	1987	No cracking, no staining	†	†	†	†	†
	1997	No cracking, no staining	NONE	0	0	0	0
213	1987	Moderate cracking, minor staining	†	†	†	†	†
	1997	Moderate cracking, minor staining	ADVANCED	6	55	0.22	3
214	1987	Moderate cracking, no staining	†	†	†	†	†
	1997	Moderate cracking, no staining	ADVANCED	6	64	0.29	3
218	1987	Moderate cracking, minor staining	†	†	†	†	†
	1997	Moderate cracking & delam, minor staining	LIGHT	4	5.8	0.22	1
219	1987	No cracking, no staining	†	†	†	†	†
	1997	No cracking, no staining	LIGHT	3	2.1	0.29	1
220	1987	No cracking, minor staining	†	†	†	†	†
	1997	No cracking, minor staining	LIGHT	4	4.0	0.27	1
221	1987	Minor cracking, no staining	†	†	†	†	†
	1997	Minor cracking, no staining	LIGHT	5	3.2	0.28	1
222	1987	Minor cracking, minor staining	†	†	†	†	†
	1997	Moderate cracking & delam, minor staining	MODERATE	5	24	0.18	2
223	1987	Severe cracking, moderate staining	†	†	†	†	†
	1997	Severe cracking & delam, moderate staining	MODERATE	6	49	0.19	2
224	1987	Extreme cracking & delam, moderate staining	†	†	†	†	†
	1997	Extreme cracking & delam, moderate staining	ADVANCED	6	45	0.26	3
225	1987	Severe cracking & delam, severe staining	†	†	†	†	†
	1997	Severe cracking & delam, moderate staining	EXTREME	6	84	0.34	4
226	1987	Extreme cracking & delam, severe staining	†	†	†	†	†
	1997	Extreme cracking & delam, severe staining	EXTREME	6	96	0.33	4
227	1987	Severe cracking & delam, severe staining	†	†	†	†	†
	1997	Severe cracking & delam, moderate staining	EXTREME	6	92	0.33	4
215	1987	Extreme cracking	†	†	†	†	†
	1997	Extreme cracking & delam, minor staining	EXTREME	6	100	0.56	4
228	1987	Extreme cracking & delam, severe staining	†	†	†	†	†
	1997	Extreme cracking & delam, moderate staining	EXTREME	6	100	0.42	4
212	1987	No cracking, no staining	†	†	†	†	†
	1997	No cracking, no staining	NONE	0	0	0	0
217	1987	No cracking, no staining	†	†	†	†	†
	1997	No cracking, no staining	NONE	0	0	0	0

\* CLASS is an incremental scale from 0 to 4, with 4 being most extreme. It is derived from the log of the multiplied product of Measured % Surface Area Affected and Maximum Pit Depth.

† Not performed as autopsies were conducted in 1997.



## *Electrochemical Corrosion Assessment*

Table 5 includes intermat resistance, concrete surface resistivity, EIS solution resistance, and Rp test results, including an apparent corrosion current density (ACD). Average intermat resistance values from the previous FHWA study<sup>(2)</sup> are listed for comparison.

The results of the intermat resistances were 86 percent greater, on average, than in the original study, with the exception of specimens 212, 223, and 228. Specimens 223 and 228 exhibited an increase in resistance by as much as 27 times the original test results. This may be attributed to separation between the upper and lower concrete lifts and to extreme cracking and delamination. Neither calcium nitrite nor chloride contents appear to have had a significant effect on the intermat resistance of the specimens.

In addition, a review of the concrete surface resistivity data does not seem to indicate any significant differences between specimens which contain calcium nitrite and all other specimens. Nor are there any apparent differences between specimens which contain chloride and the control slabs. One-third of the specimens exhibited noticeably higher resistivity values than the others, which may be attributed to cracking and delamination of these slabs due to corrosion.

Polarization resistance measurements give a relatively inverse indication of corrosion activity. These measurements were performed when the mats had been disconnected from each other for at least 2 days, so that an independent assessment of each mat could be done. An apparent corrosion current density (ACD) representative of the average conditions over the mat surface can be obtained from the measured value of Rp by applying the Stern-Geary equation to the measured values:

$$ACD = 0.026 V A_R^{-1} R_p^{-1} \quad (\text{Eq. 1})$$

where  $A_R$  is the surface area of the rebar mat (0.297 m<sup>2</sup> for the top mat and 0.511 m<sup>2</sup> for the bottom mat) and 0.026 V is an empirical value for the Stern-Geary constant commonly used for steel in concrete.<sup>(7)</sup> With the exceptions of Slabs 211, 215, and 228, the highest observed top mat ACD values (typical of those observed in actively corroding steel)<sup>(8)</sup> generally coincided with observations of severe corrosion deterioration. For slabs showing indications of top mat corrosion, the ACD values of the lower mat were typically much lower than those of the top mat. This was to be expected since chloride contamination was much more severe in the top lift.

Average potentials versus CSE for top and bottom mats and the computed potential difference between mats are included in table 6. For specimens containing calcium nitrite, the top mat potentials became more negative as the initial chloride contents increased. The bottom mat potentials in 1980-1987 followed trends comparable to those of the top mat potentials. The 1997 bottom mat potentials tended to be more positive than in 1980-1987. This change may reflect a combination of extended electrical decoupling between both mats, and of an increasing nitrite content in the bottom lift (see nitrite analysis results).

**Table 5**  
**Results From Non-Destructive Testing**

SLAB NO.	PERIOD OF TESTS	23°C INTERMAT RESISTANCE (Ω)	SURFACE RESISTIVITY (kΩ-cm)	TOP MAT Rs (Ω)	TOP MAT Rp (Ω)	TOP MAT ACD (μA/cm <sup>2</sup> )	BOTTOM MAT Rs (Ω)	BOTTOM MAT Rp (Ω)	BOTTOM MAT ACD (μA/cm <sup>2</sup> )
211	1980-1987	16.2	†	†	†	†	†	†	†
	1997	31.1	5.5	1.9	0.93	9.38	17.5	84	0.104
216	1980-1987	11.2	†	†	†	†	†	†	†
	1997	23.0	1.8	4.8	253	0.0345	11.2	136	0.064
213	1980-1987	13.3	†	†	†	†	†	†	†
	1997	24.0	113	2.6	1.2	7.27	11.4	63	0.138
214	1980-1987	13.2	†	†	†	†	†	†	†
	1997	23.6	59	3.8	1.51	5.82	13.3	78	0.112
218	1980-1987	12.4	†	†	†	†	†	†	†
	1997	28.4	10	5.3	63	0.138	13.0	52	0.168
219	1980-1987	11.0	†	†	†	†	†	†	†
	1997	27.1	10	5.1	95	0.0918	13.1	131	0.067
220	1980-1987	12.4	†	†	†	†	†	†	†
	1997	24.0	5.4	6.0	42	0.208	15.1	82	0.106
221	1980-1987	12.3	†	†	†	†	†	†	†
	1997	22.4	7.5	10.6*	64	0.136	14.5	84	0.104
222	1980-1987	15.3	†	†	†	†	†	†	†
	1997	31.7	6.4	6.0	14	0.623	12.6*	65	0.134
223	1980-1987	59.1	†	†	†	†	†	†	†
	1997	1613	7.7	3.5	0.9	9.70	123*	218	0.04
224	1980-1987	14.6	†	†	†	†	†	†	†
	1997	18.8	48	1.3*	2.8	3.12	11*	34	0.26
225	1980-1987	13.0	†	†	†	†	†	†	†
	1997	16.4	58	0.58	2.9	3.01	6.0	N/A	N/A
226	1980-1987	11.0	†	†	†	†	†	†	†
	1997	19.1	21	6.1	8.1	1.08	9.0	99	0.088
227	1980-1987	10.9	†	†	†	†	†	†	†
	1997	14.6	50	3.7	3.3	2.73	5.0	101	0.086
215	1980-1987	13.5	†	†	†	†	†	†	†
	1997	31.6	5.8	7.6*	8.54	1.02	11.0	24	0.364
228	1980-1987	63.5	†	†	†	†	†	†	†
	1997	711	35	18.5	25	0.349	999*	619	0.14
212	1980-1987	133	†	†	†	†	†	†	†
	1997	107.8	9.1	2.0	N/A	N/A	87	368	0.024
217	1980-1987	13.0	†	†	†	†	†	†	†
	1997	23.1	5.2	4.9	N/A	N/A	15.5	71	0.123

Note: Values from the 1980-1987 test period are an average of all readings taken during that 2,429-day period.<sup>(2)</sup>

\* These solution resistance values are calculated using data from polarization resistance testing.

† Not performed in 1980-1987.

**Table 6**  
**Reinforcement Mat Potentials Versus CSE and Computed Potential Differences Between Mats**

SLAB NO.	Ca(NO <sub>3</sub> ) <sub>2</sub> ADMIXED	PERIOD OF MEASUREMENT	CSE POTENTIALS (mV)*		TOP vs. BOTTOM POTENTIAL DIFFERENCE (mV)
			TOP MAT	BOTTOM MAT	
211		1980-1987	-111	-76	-35
		1997	-141	-57	-84
216	✓	1980-1987	-105	-106	1
		1997	-30	-18	-12
213		1980-1987	-219	-145	-74
		1997	-140	71	-211
214		1980-1987	-300	-156	-144
		1997	-128	74	-202
218	✓	1980-1987	-185	-174	-11
		1997	-122	-39	-83
219	✓	1980-1987	-174	-191	17
		1997	-74	41	-115
220	✓	1980-1987	-215	-180	-35
		1997	-139	-63	-76
221	✓	1980-1987	-181	-189	8
		1997	-164	-51	-113
222	✓	1980-1987	-297	-245	-52
		1997	-286	-42	-244
223	✓	1980-1987	-369	-220	-149
		1997	-293	17	-310
224	✓	1980-1987	-370	-284	-86
		1997	-346	-15	-331
225	✓	1980-1987	-406	-285	-121
		1997	-321	56	-377
226	✓	1980-1987	-408	-297	-111
		1997	-338	44	-382
227	✓	1980-1987	-418	-291	-127
		1997	-250	-33	-217
215		1980-1987	-393	-289	-104
		1997	-354	-335	-19
228	✓	1980-1987	-411	-300	-111
		1997	-446	-23	-423
212		1980-1987	-154	-38	-116
		1997	-117	-106	-11
217	✓	1980-1987	-117	-96	-21
		1997	-69	-46	-23

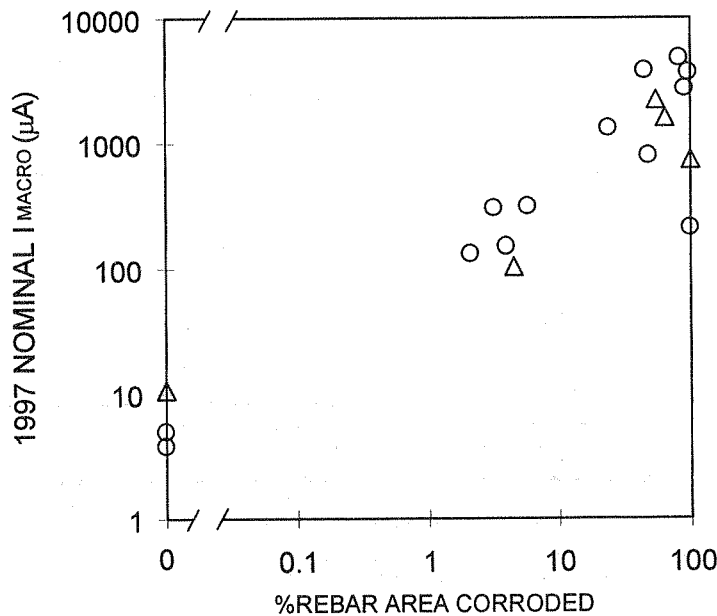
\* Potentials for 1980-1987 are an average of all measurements obtained during that study period.<sup>(2)</sup>

Table 7 summarizes the corrosion data for the 18 FHWA specimens. In order to account for temperature differences throughout the duration of the project, all current and intermat resistance measurements were adjusted to 23°C in the manner of Report No. FHWA-RD-83-012<sup>(3)</sup> utilizing the following equations:

$$I_{23^{\circ}\text{C}} = \frac{I_{\text{ambient}}}{e^{\left[2883\left(\frac{1}{T_{23^{\circ}\text{C}}} - \frac{1}{T_{\text{ambient}}}\right)\right]}} \quad (\text{Eq. 2})$$

$$R_{23^{\circ}\text{C}} = R_{\text{ambient}} e^{\left[2883\left(\frac{1}{T_{23^{\circ}\text{C}}} - \frac{1}{T_{\text{ambient}}}\right)\right]} \quad (\text{Eq. 3})$$

Specimen driving voltage listed for 1997 was calculated as the product of the 1997 values obtained for the nominal macrocell current and intermat resistance. The driving voltage values listed for the 1980-1987 period for each slab are an average of the values obtained during that period by disconnecting the top and bottom mats and measuring the potential difference immediately afterwards.<sup>(2)</sup> In general, the nominal macrocell currents obtained in 1997 were comparable to the weighted-average macrocell current reported for the 1980-1987 period.<sup>(2)</sup> Exceptions were high chloride slabs 215 and 228, which showed much lower currents than those reported in the earlier study. Those reductions may have resulted from physical slab deterioration. Taking into account those exceptions, figure 6 shows that there was also good correlation between the nominal macrocell currents obtained in 1997 and the percent of rebar surface area affected by corrosion (table 4) observed in the subsequent 1997 destructive examination.



**Figure 6 - Nominal macrocell current measured in 1997 as a function of percentage of rebar affected by corrosion. [(Δ) Slabs with no admixed nitrite; (○) Slabs with admixed nitrite.]**

Corrosion macrocell current data are not available for the 1987-1997 period, during which the external electrical connection in many slabs was also lost and severe concrete deterioration affected some slabs. Nevertheless, for the purposes of comparison, a nominal weighted-average macrocell current (NWMC) for the period 1980-1997 was assigned to each slab. This was implemented by assuming that external connection existed for most of the 1980-1997 period; that the 10-minute currents measured in 1997 roughly approximate the corresponding steady-state current at that time; and that the current varied linearly with time between 1987 and 1997, starting with a value equal to the weighted 1980-1987 average. The resulting NWMC value for each slab is listed in table 7, and it generally parallels the trends obtained during 1980-1987.

The actual 1980-1987 macrocell currents and 1980-1997 NWMC were integrated over their respective time periods and converted into theoretical amounts of iron consumed, assuming oxidation to ferrous ions, by the Faradaic factor 1.04 g/A-h. <sup>(2-3)</sup> It must be emphasized that these amounts can only correspond to the added corrosion at the top mat due to macrocell coupling to the bottom mat. These amounts should be added to any local cell corrosion supported by cathodic reactions at the top mat; that local cell action can be substantial, as indicated by the polarization resistance measurements discussed earlier. However, both macrocell and local cell currents are expected to be indicative of conditions promoting overall corrosion action. This is confirmed by examining figure 7, in which the NWMC (converted into current density by dividing into the top mat rebar area, 0.297 m<sup>2</sup>) is compared with the ACD from polarization resistance measurements; the slabs having the highest macrocell action generally also showed the highest ACD, with the exception of slabs 211, 215, and 228 as previously indicated. Overall, the NWMC tended to be smaller than the ACD, as expected from the above discussion. The ACD values and macrocell currents (as well as the corresponding theoretical iron consumption) also generally correlated with the visual and measured rebar conditions indicated in table 4.

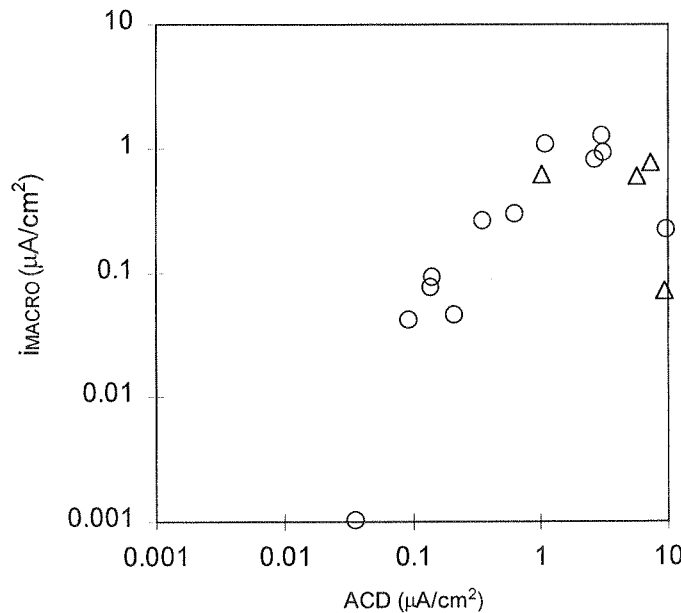


**Figure 7 - 1980-1997 nominal macrocell current density as a function of top mat apparent corrosion current density from 1997 polarization resistance measurements. [(Δ) Slabs with no admixed nitrite; (○) Slabs with admixed nitrite.]**

**Table 7**  
**Macrocell Current and Theoretical Iron Consumed**

SLAB NO.	Ca(NO <sub>3</sub> ) <sub>2</sub> ADMIXED	DATE	CONCRETE Cl CONTENT* (kg/m <sup>3</sup> )	PERIOD/ DATE	23°C INTERMAT RESISTANCE (Ω)	DRIVING VOLTAGE*** (mV)	23°C NOMINAL MACROCELL CURRENT (μA)	PERIOD	23°C WEIGHTED MACROCELL CURRENT (μA)	THEOR. IRON CONSUMED (g)
211		1980	2.1	1980-1987	16.3	7	—	1980-1987	376	22.8
		1997	2.0	1997	21.8	2.2	71	1980-1997**	284	43.7
216	✓	1980	2.2	1980-1987	11.2	0	—	1980-1987	2	0.09
		1997	2.0	1997	16.1	0.06	2.7	1980-1997**	2.2	0.42
213		1980	4.7	1980-1987	13.3	34	—	1980-1987	2296	139
		1997	1.6	1997	16.8	37	1548	1980-1997**	2069	238
214		1980	4.1	1980-1987	13.2	36	—	1980-1987	2050	124
		1997	2.3	1997	16.5	26	1105	1980-1997**	1477	228
218	✓	1980	5.0	1980-1987	12.4	3	—	1980-1987	231	14.0
		1997	3.7	1997	19.9	4.5	160	1980-1997**	188	29.0
219	✓	1980	5.0	1980-1987	11	2	—	1980-1987	115	6.97
		1997	3.8	1997	19	2.2	81	1980-1997**	94	14.5
220	✓	1980	6.9	1980-1987	12.4	3	—	1980-1987	112	6.77
		1997	4.4	1997	16.8	2.5	104	1980-1997**	107	16.5
221	✓	1980	6.5	1980-1987	12.3	3	—	1980-1987	113	6.87
		1997	5.5	1997	15.7	4.7	208	1980-1997**	171	26.3
222	✓	1980	7.9	1980-1987	15.3	6	—	1980-1987	216	13.1
		1997	6.3	1997	22.2	29	914	1980-1997**	639	98.4
223	✓	1980	8.5	1980-1987	59.1	27	—	1980-1987	476	22.8
		1997	6.4	1997	1130	897	555	1980-1997**	525	80.7
224	✓	1980	9.9	1980-1987	14.6	25	—	1980-1987	1152	69.9
		1997	4.4	1997	13.2	50	2668	1980-1997**	2071	320
225	✓	1980	9.7	1980-1987	13.0	41	—	1980-1987	2117	128
		1997	3.5	1997	11.5	54	3315	1980-1997**	2843	438
226	✓	1980	10.0	1980-1987	11	40	—	1980-1987	2591	157
		1997	2.1	1997	13.4	49	2571	1980-1997**	2579	397
227	✓	1980	12.0	1980-1987	10.9	31	—	1980-1987	1877	114
		1997	2.3	1997	10.2	28	1911	1980-1997**	1898	292
215		1980	13.8	1980-1987	13.5	51	—	1980-1987	3566	216
		1997	9.6	1997	22.1	10	318	1980-1997**	1597	246
228	✓	1980	13.4	1980-1987	63.5	58	—	1980-1987	1663	101
		1997	7.2	1997	498	105	148	1980-1997**	744	115
212		1980	0.0	1980-1987	133	0	—	1980-1987	7	0.42
		1997	0.2	1997	75.5	0.8	7.5	1980-1997**	7.3	1.12
217	✓	1980	0.0	1980-1987	13	0	—	1980-1987	0	0
		1997	0.2	1997	16.2	0.08	3.4	1980-1997**	2.1	0.32

\* Concrete chloride concentrations at the depth of the top reinforcement mat.

\*\* The 1980-1997 values are presented as NWMC.

\*\*\* The 1997 result is a calculated value.

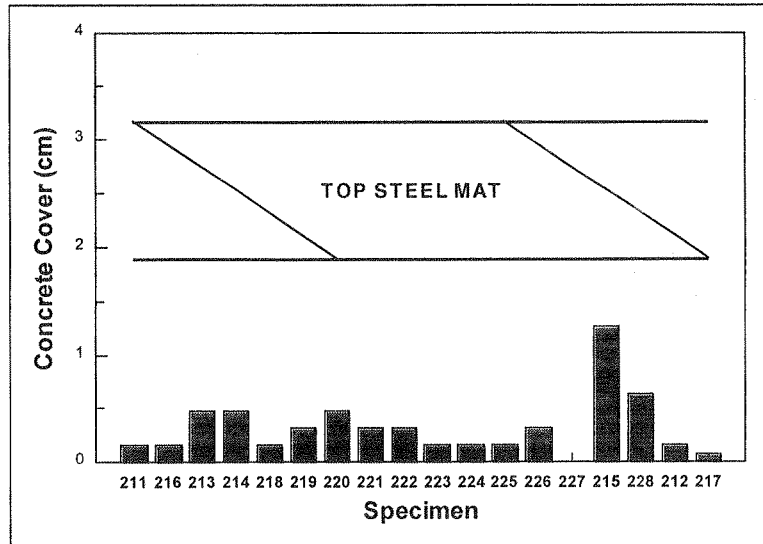


Figure 8 - Carbonation depth for all specimens.

*Concrete Carbonation, Chloride, and Nitrite Analysis*

Carbonation depth measurements are shown in figure 8. With the exception of specimens 211 and 216, the average ratio of carbonation depth in specimens without nitrites to that in comparable specimens with nitrites was 2 to 1. Table 8 includes carbonation depth, measured chloride content at top mat depth, and total and free nitrite concentrations at top mat depth obtained from destructive testing of the specimens, in addition to the measured chloride to free nitrite ratio.

Figure 9 shows the chloride concentration measured at the top bar level of each specimen in 1980 after ponding and in 1997, as well as initially admixed chloride content. The chloride profiles determined for seven specimens are displayed in figure 10. The results in figures 9 and 10 are generally consistent with expected behavior. The

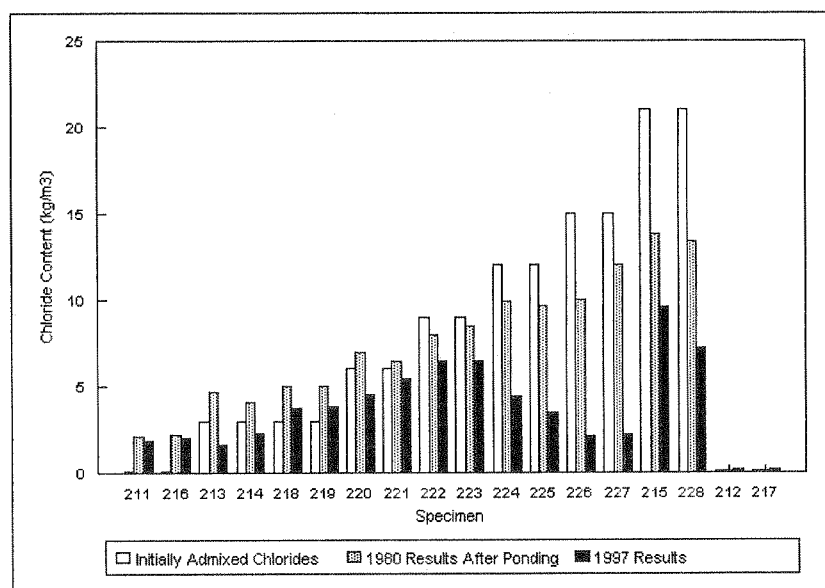


Figure 9 - History of chloride content at top rebar mat for all specimens.

**Table 8**  
**Results From Destructive Testing**

SLAB No.	DESCRIPTION*	CARB DEPTH (cm)	MEASURED CHLORIDE** (kg/m <sup>3</sup> )	TOTAL NITRITE** (kg/m <sup>3</sup> )	FREE NITRITE** (ppm)	NO <sub>2</sub> /Cl RATIO**
211	0 CN, 0 Cl, P	0.16	2.0			
216	10.7 CN, 0 Cl, P	0.16	2.0	3.72	8370	1.86
213	0 CN, 3 Cl, P	0.48	1.6			
214	0 CN, 3 Cl, P	0.48	2.3			
218	10.7 CN, 3 Cl, P	0.16	3.7		4620	
219	10.7 CN, 3 Cl, P	0.32	3.8	4.47	6350	1.18
220	10.7 CN, 6 Cl, P	0.48	4.4	5.21		1.16
221	10.7 CN, 6 Cl, P	0.32	5.5		7530	
222	10.7 CN, 9 Cl, P	0.32	6.3		9370	
223	10.7 CN, 9 Cl, P	0.16	6.4	3.57		0.56
224	10.7 CN, 12 Cl, P	0.16	4.4	1.63		0.37
225	10.7 CN, 12 Cl, P	0.16	3.5			
226	10.7 CN, 15 Cl, P	0 to 0.32	2.1	0.62		0.30
227	10.7 CN, 15 Cl, P	0	2.3			
215	0 CN, 21 Cl, P	0.16 to 1.27	9.6			
228	10.7 CN, 21 Cl, P	0.16 to 0.64	7.2	1.16		0.16
212	0 CN, 0 Cl, NP	0.16	0.2			
217	10.7 CN, 0 Cl, NP	0.08	0.2	4.81	6260	24.1

\* CN - Calcium Nitrite, P - Poned, NP - Not Poned, Admixed amounts given in kg/m<sup>3</sup>

\*\* Tests conducted on concrete at top mat depth (figure 4).

top lift chloride concentrations measured in 1980 in specimens with no initially admixed chloride reflect chloride acquired during ponding. Specimens with admixed chloride showed a 1980 chloride content roughly proportional to the admixed amount. For specimens with less than 10 kg/m<sup>3</sup> admixed chloride, the chloride content in the top lift was somewhat lower than that measured in 1980. Examination of figure 10 suggests that the change can be explained by chloride diffusion into the lower lift, which did not have chlorides initially. The initial chloride profile (which had a sharp step down to near zero concentration at the transition from the top to the bottom lifts) relaxed over a period  $t \approx 15$  years into the patterns shown in figure 10. The observed final profiles correspond roughly to a characteristic diffusion distance  $x$  equal to about 1/2 of the slab thickness, or 7.5 cm. In simple diffusion processes,<sup>(9)</sup>  $x$  is on the order of  $(Dt)^{1/2}$ , where  $D$  is the diffusion coefficient. Thus, the results would indicate an apparent chloride diffusion coefficient of about 5 cm<sup>2</sup>/yr, which is consistent with observations of chloride diffusivity in concrete with high w/c ratios.<sup>(9)</sup> A more sophisticated analysis would need to consider chloride interactions with other mobile species in the concrete (especially the nitrite), and transport mechanisms beyond diffusion.

For specimens 222-227 (with high admixed chloride content), the chloride concentration in the top lift was markedly lower in 1997 than in 1980 (figure 9). This change is too large to be explained by the amount diffused into the bottom lift (see the trends for selected slabs in figure 10). Examination of table 4 reveals that those slabs with high admixed chlorides and the greatest top lift chloride loss were also those with the most



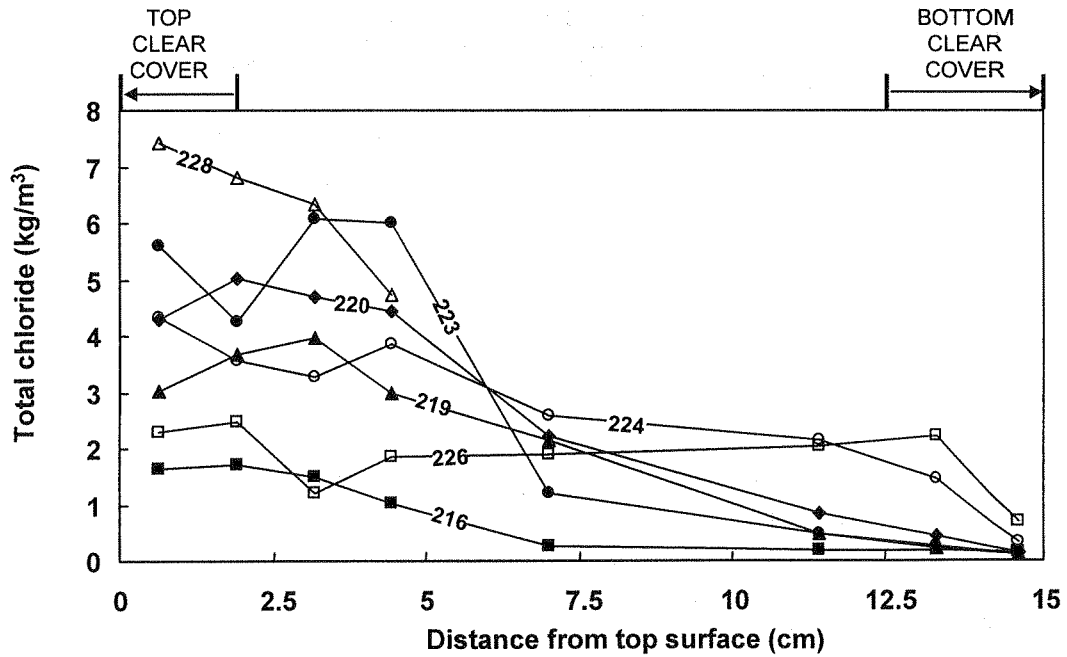


Figure 10 - Profiles of total chlorides incrementally measured through the thickness of seven specimens (specimen number indicated for each profile).

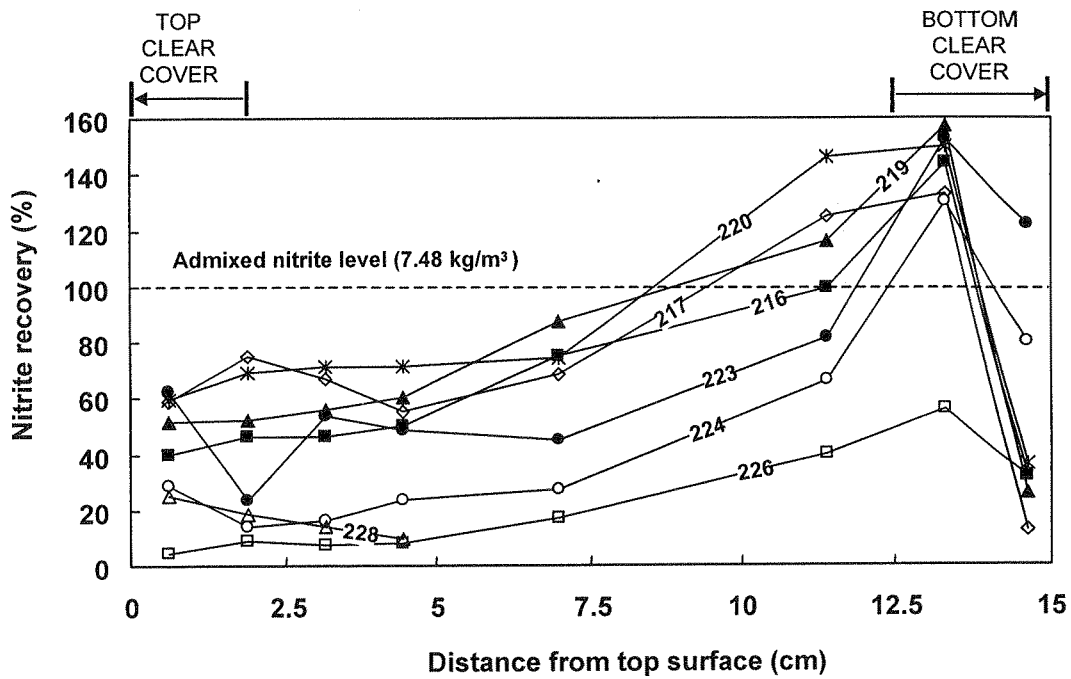


Figure 11 - Profiles of total measured nitrites as a percentage of the originally admixed nitrites for eight specimens (specimen number indicated for each profile).

severe concrete cover deterioration. Thus, it is likely that much of the chloride loss in the top lift of these slabs was due to rainwater leaching facilitated by cracks during years of weather exposure.

Figure 11 illustrates the results for total nitrite content of the concrete slabs under investigation. The recovery percentage reported is the total extracted nitrite (from the two-step extraction method described above) divided by the originally admixed nitrite (see Appendix B). Initially, both lifts had the same nitrite content.

Separate tests with freshly made specimens showed that the extraction method employed here was able to extract 95 to 100 percent of the total nitrite from the concrete. To verify the accuracy of the test method, unused portions of the concrete powder samples from six slabs, used to obtain the data in figure 11, were selected to span a wide range of measured total nitrite contents. Those portions were independently analyzed again in blind tests by W.R. Grace & Co., with the results being displayed in figure 12. The results from the method used in this work matched those from the W.R. Grace & Co. laboratory very well, with an  $R^2$  value of 0.9967. Nitrite recovery was generally about 5 percent higher than that reported by W.R. Grace & Co.; this 5 percent difference is likely the result of the long-term second extraction.

An estimate was made of the total amount of nitrite present throughout the entire thickness of each slab by numerically integrating each of the profiles in figure 11. Separate integrations for the top and bottom lifts were also conducted. For slabs not experiencing severe cover deterioration, the integrated nitrite content of the top lift was between  $\frac{1}{2}$  and  $\frac{2}{3}$  of the original admixed amount, while in the bottom lift, the analysis showed about  $\frac{1}{3}$  greater nitrite than admixed. The top plus bottom lift average content in those slabs was at least  $\frac{3}{4}$  of the initially admixed amount. Thus, much of the initially admixed nitrite appears to have remained within the slabs, but redistributed along the slab thickness in a manner opposite to that of the final chloride profile.

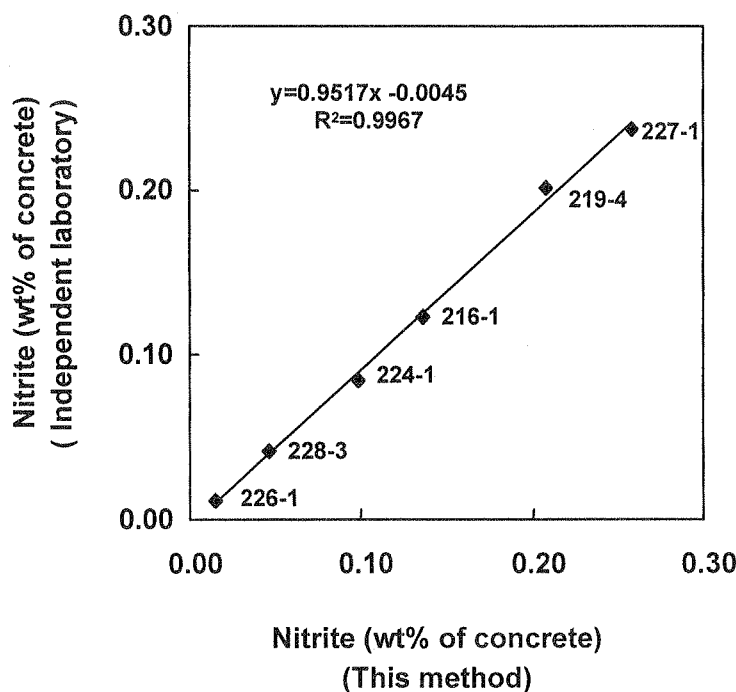


Figure 12 - Comparison of nitrite analysis results obtained with the method used in this work and by an independent laboratory. [The numbers identify the slab and slice number (figure 11, counting from left) from which the powder originated.]

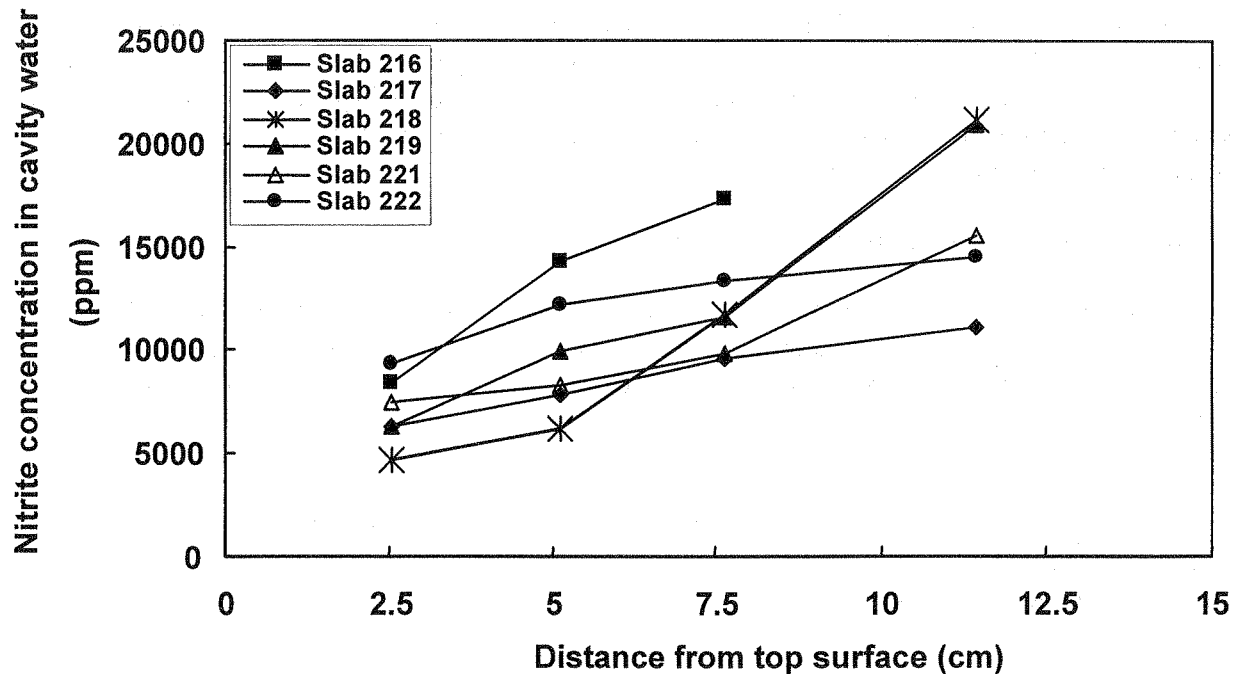


Figure 13 - Profiles of free nitrites as measured in cavity water for six specimens.

For the slabs with extensive cover damage, the nitrite content in the top lift was much lower than the nominal admixed amount. The concentration in these slabs nevertheless increased markedly toward the bottom lift, where in two instances, values exceeded the nominal admixed amount.

The free nitrite measurements are shown in figure 13. In the locations investigated, the free nitrite values increased with distance from the top surface, generally following the trends shown in figure 11 for the total nitrites. The free nitrite content was roughly proportional to the total nitrite content, on average about 8,000 ppm free nitrite for every 4 kg/m<sup>3</sup> of total nitrite. If the concrete had about 10 percent capillary volume porosity, this proportionality would indicate that about 1/5 of the total nitrite was dissolved in the pore solution, while the remaining 4/5 were bound in another form in the concrete (see Appendix B for an example calculation). This binding is reversible, since nearly all the nitrite was readily extracted when the concrete was leached with large amounts of water in the procedure used for total nitrite analysis.

The low amount of nitrite observed in the top lift of slabs that had high admixed chlorides is likely the result of rainwater leachout from the heavily damaged concrete, as it is thought to be the case for chloride ions in the same slabs. This is supported by measurements that have shown that diffusivity of nitrite and leaching kinetics are comparable to those of chloride.<sup>(10)</sup> Alternatively, some nitrite may have been consumed by reaction with Fe<sup>2+</sup>-based corrosion products.<sup>(3)</sup> The reason for the increase in nitrite toward the bottom in most of the slabs is not known at present. Barring concentration gradients introduced at the time of casting, the increase at the bottom occurred during the life of the slabs and coincided with the downward diffusional transport of chloride from the top to the bottom lift. The possibility of a coupled ionic transport mechanism at work or of competitive binding of chlorides and nitrites should be investigated further.

The above results indicate nevertheless that much of the nominally admixed nitrite remained in the slabs that were physically sound at the end of nearly two decades of weather exposure, even though the concrete used had a w/c ratio of 0.53 and could be expected to be of relatively high permeability. On the other hand, nitrite redistribution toward the lower lift took some inhibitor away from the area of highest chloride contamination. Future investigations should be directed to determine to which extent these effects take place in the less permeable concretes regularly used for highway structures.

### *Effect of Calcium Nitrite on Corrosion Performance*

Calcium nitrite is expected to increase the steel resistance to passivity breakdown, thus resulting in an increase in the critical chloride concentration threshold  $C_T$  for corrosion initiation. Previous investigators<sup>(2,11)</sup> proposed that nitrite addition caused an increase in  $C_T$  (expressed in mass per unit volume of concrete) roughly equal to the amount of nitrite present in the concrete surrounding the reinforcing steel. The following discussion examines that interpretation in light of the present findings.

The exposure history of the tested slabs suggests that the chloride content of the concrete next to the top mat steel reached a peak some time after the ponding period ended, followed by long-term drop-off. Thus, opportunity for corrosion initiation was likely highest early in the life of the slabs unless long-term nitrite loss caused a proportionally greater loss of protection afterwards. The latter does not seem to have been the case since comparison of the 1987 and 1997 slab surveys indicates that most corrosion had already initiated in the earlier period. Thus, the presence or absence of corrosion in the slabs resulted from the occurrence of either a peak or a relatively stable level of chloride contamination, as opposed to conditions in actual service where a progressive chloride content increase with time would be more likely.

With the exception of highly contaminated slabs, corrosion both in slabs with and without nitrite did not affect the entire steel surface. Visual examination in 1997 often showed rust-covered segments alternating with uncorroded sections of rebar still showing the initial mill scale. Since chloride contamination and nitrite content at the rebar depth are expected to have shown only moderate spatial variability, the results suggest  $C_T$  varied from point to point over the rebar assembly. Proposed causes for spatial variations of  $C_T$  include changes in the local half-cell potential after adjacent areas become active,<sup>(12)</sup> local physical and chemical concrete properties,<sup>(13-14)</sup> variability of the steel surface condition,<sup>(15)</sup> and the presence of crevices and occlusions.<sup>(16)</sup> Regardless of the cause, evaluation of the inhibitor effect must take into consideration the variability of the response.

The corrosion response based on the direct observation (table 4) will be examined first. The severity of externally observable concrete deterioration and rebar corrosion followed similar trends, which may be conveniently expressed quantitatively by the percentage of rebar surface area (%RAC) affected by corrosion. Figure 14 shows the %RAC as a function of chloride content measured at the top mat depth in 1980 immediately after the end of the ponding period, hereafter called the 1980 chloride. The results for the nitrite-containing slabs followed an S-curve trend. The solid line approximating that trend corresponds to a cumulative normal distribution calculated to have the best least-square-error fit to the nitrite slab data. The results for the nitrite-free slabs are few, but appear to follow a trend similar to that of the nitrite slabs, only displaced to the left reflecting a beneficial effect of the nitrite presence. Consequently, the dashed line was constructed by laterally displacing the solid line until a best least-square-error fit to the nitrite-free slab data was obtained. That condition was achieved for a displacement amounting to 4.8 kg/m<sup>3</sup>. This mathematical procedure served the purpose of reproducibly defining a displacement between both data distributions. However, it must be emphasized that the functional form adopted for the curves was chosen for convenience in representing the trend of the data.

The beneficial effect of nitrite was manifested also when quantifying corrosion by indirect electrochemical assessment. Figure 15 shows the weighted-average macrocell current densities for the 1980-1987 and 1980-1997 (nominal) periods as a function of 1980 chloride. The results for 1980 chloride  $> 10 \text{ kg/m}^3$  show considerable experimental scatter, likely due to physical slab degradation. Nevertheless, the results for 1980 chloride  $< 10 \text{ kg/m}^3$  suggest reasonably well-defined trends, paralleling the behavior observed in figure 14. The solid and dashed lines were constructed, as in figure 14, to fit the current density data for the 1980-1987 period. The lines are offset by  $5.6 \text{ kg/m}^3$  in approximate agreement with the result from the %RAC analysis. Experimental scatter was too great to perform similar quantitative assessments using half-cell potentials or polarization resistance results. Nonetheless, the general agreement observed between the results of those methods and macrocell currents (as indicated in an earlier section) lends support to the use of the latter for this purpose.

As a first approximation, the chloride levels measured at the end of the ponding period may be considered to be representative of the peak conditions mentioned above. Figures 14 and 15 suggest that except for a parallel offset, the corrosion response to the chloride content of nitrite and nitrite-free slabs appeared to be quite similar. The effect of admixing  $7.48 \text{ kg/m}^3$  nitrite can then be interpreted as increasing the distributed values of  $C_T$  by a value in the range of  $4.8 \text{ kg/m}^3$  to  $5.6 \text{ kg/m}^3$  ( $5.2 \text{ kg/m}^3$  average). This amount corresponds to about 70 percent of the admixed nitrite content, but the actual amount of inhibitor present at the rebar level at the time of corrosion initiation was likely less than the admixed amount. This is to be expected since some migration of inhibitor to the lower lift (figure 11) must have already taken place during the first few months. In addition, nitrite leaching into the ponding water from the permeable 0.53 w/c concrete may have also reduced the nitrite below the admixed levels by the end of ponding (a likely explanation also for chloride contents less

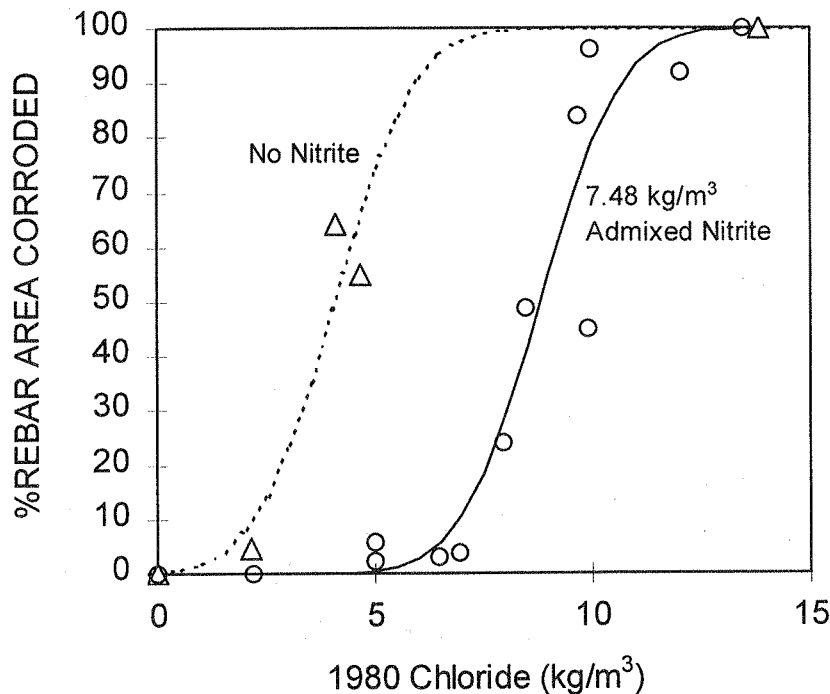


Figure 14 - Percentage of rebar surface area affected by corrosion as a function of top mat chloride content at the end of the ponding period. [(Δ) Slabs with no admixed nitrite; (○) Slabs with admixed nitrite. See text for procedure to obtain trend lines.]

than the admixed amount in some of the high chloride slabs, figure 9). If the reduction caused nitrite levels to drop to about 70 percent of the admixed amount by the time corrosion initiation took place, then the results would support earlier reports of an elevation of  $C_T$  in a 1:1 proportion by weight of nitrite.

Data on top mat nitrite content at the end of the ponding period are not available to compare directly with the chloride measurements at that time. However, the extent of corrosion can be examined as a function of the relative nitrite and chloride amounts measured at the time of the 1997 autopsies. These results were not analyzed in the same manner as performed in figure 14 for the earlier 1980 data, because the relatively large slab-to-slab variations in 1997 nitrite content would make comparison difficult. Instead, the extent of corrosion was examined as a function of the difference between nitrite and chloride concentrations measured for each slab in 1997, in an attempt to reveal changes when the difference became zero (equal remaining amounts of nitrite and chloride). This analysis is shown in figure 16 for the %RAC. The graph shows that severe corrosion was observed only for slabs where the 1997 chloride content was greater than the 1997 nitrite content. The results for the slabs without admixed nitrite are plotted in the same manner (since nitrite content was zero, the abscissa in those cases is simply the negative of the chloride content). Both data sets roughly overlap, suggesting that nitrite canceled the effect of an approximately equal amount of chloride up to the time of autopsy. Figure 17 shows a similar representation for the weighted-average macrocell current densities, also exhibiting signs of severe macrocell action only when chlorides exceeded nitrites and overlapped the results from slabs without admixed nitrite. Although the species concentrations are only those at the end of the 17-year exposure, the results generally support the interpretation that corrosion thresholds increase by an amount roughly equal to the nitrite concentration.

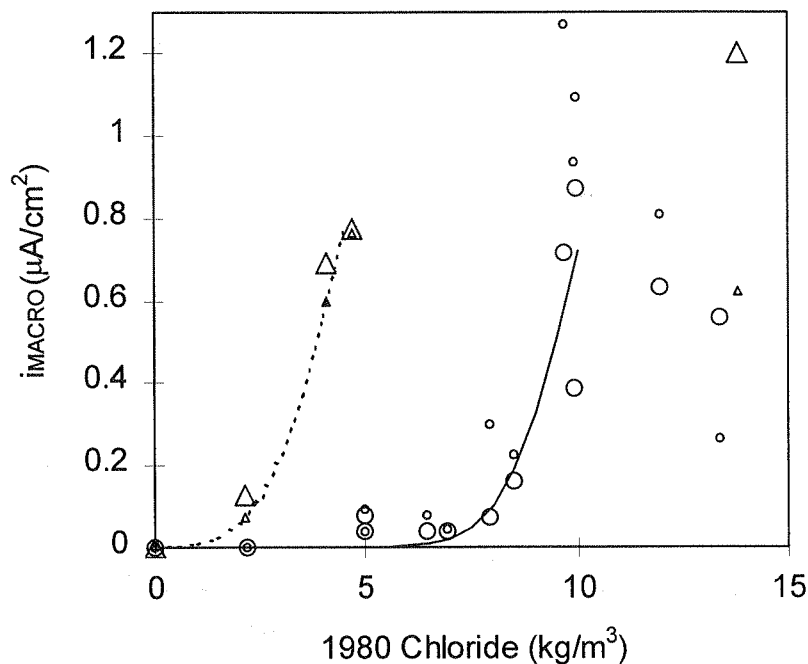
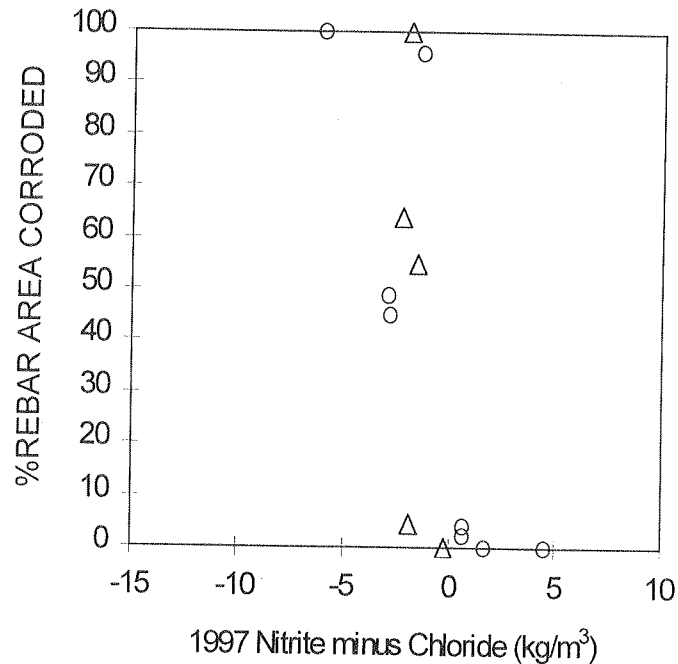


Figure 15 - Macrocell current density as a function of top mat chloride content at the end of the ponding period. [( $\Delta$ ) Slabs with no admixed nitrite, 1980-87; ( $\blacktriangle$ ) Slabs with no admixed nitrite, 1980-97 nominal values; ( $\circ$ ) Slabs with admixed nitrite, 1980-87; ( $\bullet$ ) Slabs with admixed nitrite, 1980-97 nominal values. See text for procedure used to obtain trend lines, which apply only to the results for 1980-87 and concentrations less than 10 kg/m<sup>3</sup>.]



**Figure 16 - Percentage of rebar surface area affected by corrosion as a function of top mat 1997 nitrite content minus 1997 chloride content. [(  $\Delta$  ) Slabs with no admixed nitrite; (  $\circ$  ) Slabs with admixed nitrite.]**

The above findings suggest that slabs with top mat nitrite content consistently higher than the chloride content should be nearly free from corrosion, as in the chloride- and nitrite-free slabs. This was confirmed in Slab 216, which had about 2 kg/m<sup>3</sup> chloride at the end of the ponding period (as well as in 1997) and still retained 3.7 kg/m<sup>3</sup> top mat nitrite in 1997. Slab 216 showed virtually completely passive steel behavior, either by direct observation or by electrochemical indicators. In contrast, nitrite-free Slab 211 that also had about 2 kg/m<sup>3</sup> chloride at the end of the ponding period showed rebar corrosion on 4.5 percent of its surface and moderate electrochemical indications of corrosion. However, nitrite-containing slabs with nearly equal nitrite and chloride amounts did not show complete corrosion suppression. This was the case with slabs 218 and 219, which had 1980 chloride amounts of about 5 kg/m<sup>3</sup> (comparable to the likely nitrite content at the top mat level at that time), and retained (Slab 219) some nitrite excess when analyzed at the end of the investigation. Slab 219 showed minor corrosion on a level comparable to that of nitrite-free, low chloride Slab 211. Slab 218, twin of 219, showed moderate corrosion, including some concrete cracking. Both Slabs 218 and 219 also showed moderate electrochemical indications of corrosion. Slabs 220 and 221 also did not show complete corrosion suppression, but that is not surprising since these slabs had about 2 kg/m<sup>3</sup> higher 1980 chloride contents than Slabs 218 and 219, while having the same admixed nitrite amounts.

The overall results of this investigation indicate beneficial effects of nitrite presence, approximately counteracting the effects of chloride content on a 1:1 weight basis in the concentration range investigated. That interpretation was well confirmed by no evidence of active corrosion in a low chloride contamination case (Slab 216), and by reduction of corrosion severity in cases where some corrosion existed. However, experimental data were unavailable in important situations of interest, for example, cases with chloride contents of several kg/m<sup>3</sup> and actual nitrite contents one or two kg/m<sup>3</sup> higher. Future work will be needed to establish whether highly efficient corrosion suppression takes place also under those conditions.

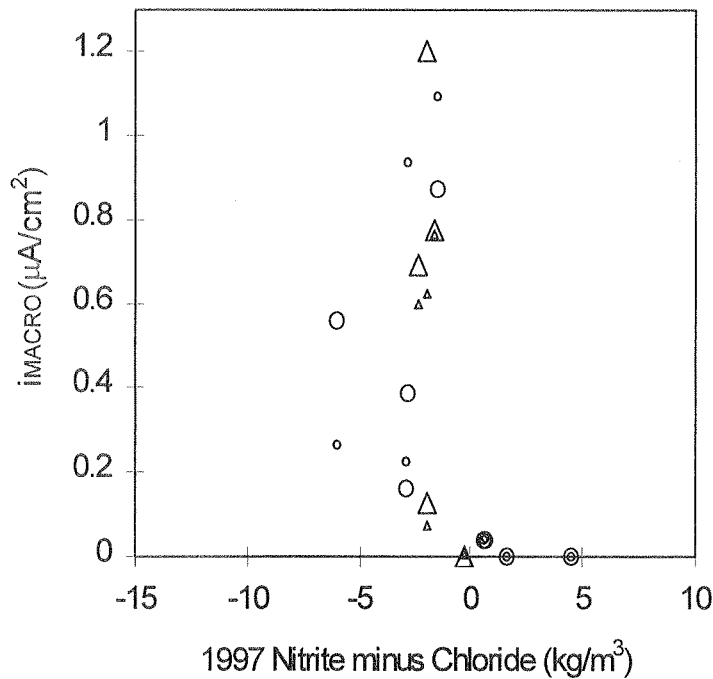


Figure 17 - Macrocell current density as a function of top mat 1997 nitrite content minus 1997 chloride content. [ (△) Slabs with no admixed nitrite, 1980-87; (△) Slabs with no admixed nitrite, 1980-97 nominal values; (○) Slabs with admixed nitrite, 1980-87; (○) Slabs with admixed nitrite, 1980-97 nominal values.]

The investigation showed also that nitrite remained as a chemically identifiable admixture after 17 years in the concrete environment. The analyses showed also that a large fraction of the admixed inhibitor in sound slabs remained in place after leaching during the initial ponding and 17 years weather exposure. The nitrite loss was moderate considering the highly permeable concrete used, and the prognosis for long-term nitrite retention in physically sound higher density concretes appears to be good. The investigation also showed significant nitrite loss from physically deteriorated concrete. This loss is expected to reduce the extent of any residual protection during the propagation stages of corrosion.

## CONCLUSIONS

1. In general, information obtained from all corrosion measurement techniques applied in this study correlates well with the visual survey of the concrete surface and the extracted reinforcing steel. The non-destructive corrosion measurement techniques employed by this study (particularly half-cell potential and macrocell current) are useful in evaluating the condition of a reinforced concrete specimen with initially added calcium nitrite.
2. The physical appearance of the slabs at 17 years resembled that observed at 7 years. The measurement trends observed during the first 7 years of testing generally agreed with the corrosion condition at 17 years.



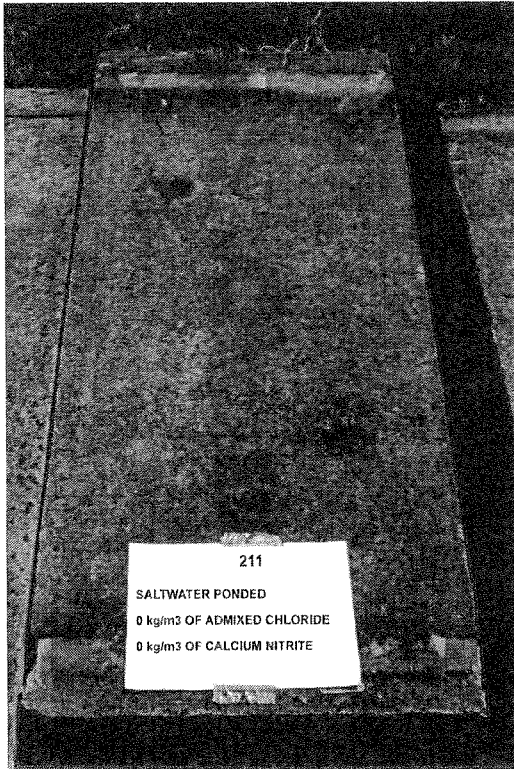
3. The nitrite amount ( $\text{kg/m}^3 \text{NO}_2^-$ ) remaining in the concrete approximately counteracted the corrosion effects of an equal amount of chloride ( $\text{kg/m}^3 \text{Cl}^-$ ) in the concentration range investigated. No evidence of active corrosion was observed when nitrite was well in excess of the chloride content, but that result needs to be demonstrated for a wider range of chloride and nitrite contents.
4. After 17 years, nitrite that remains in the concrete resides in a chemically stable form and retains its corrosion-inhibiting characteristics.
5. Small-cavity measurements indicated that nitrite is present in the pore solution to a concentration of several thousand ppm when admixed at  $7.48 \text{ kg/m}^3$ . Measurements of samples with various levels of total nitrite content suggest that about 1/5 of the total nitrite was present in the pores of the concrete (at 100 percent relative humidity), while the rest was reversibly bound in another form in the concrete.
6. Even though the concrete had a high w/c ratio (0.53), nitrite escape from physically sound slabs exposed to 46 days initial ponding and 17 years weathering was moderate. However, concentration profile measurements indicated that some of the nitrite had redistributed toward the bottom of the slabs, thereby lessening the protection available for the top mat. Chloride ion had also redistributed toward the bottom as expected, since the bottom lift was originally chloride free. The cause of the nitrite redistribution (and whether it is related to the chloride transport) was not determined.
7. Significant nitrite and chloride loss took place in the top lift of slabs that had suffered extensive physical deterioration. It is expected that the losses were at least due, in part, to leaching from ponding and weathering (and possibly reaction with iron corrosion products for the nitrite).

## REFERENCES

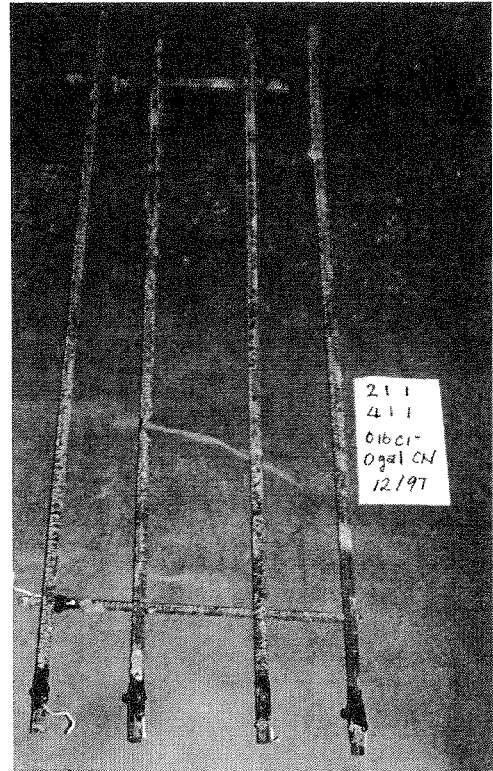
1. A.M. Rosenberg, J.M. Gaidis, T.G. Kossivas, and R.W. Previtte, "A Corrosion Inhibitor Formulated With Calcium Nitrite for Use in Reinforced Concrete," 1977, *Chloride Corrosion in Concrete*, ASTM STP 629, American Society for Testing and Materials, pp. 89-99.
2. Y.P. Virmani, *Time-to-Corrosion of Reinforcing Steel in Concrete Slabs, Volume 6*, 1988, Federal Highway Administration, Publication No. FHWA-RD-88-165.
3. Y.P. Virmani, *Time-to-Corrosion of Reinforcing Steel in Concrete, Volume 5*, 1983, Federal Highway Administration, Publication No. FHWA-RD-83-012.
4. Florida Department of Transportation, "Determining Low Levels of Chlorides in Concrete and Raw Materials," 1994, *Manual of Florida Sampling and Testing Methods*, FM 5-516.
5. Lianfang Li, A.A. Sagiés, and Noreen Poor, "In-Situ Leaching Investigation of pH and Nitrite Concentration in Concrete Pore Solution," *Cement and Concrete Research*, Vol. 29, 1999 (in press).
6. A.A. Sagiés, E.I. Moreno, and C. Andrade, "Evolution of pH During In-Situ Leaching in Small Concrete Cavities," *Cement and Concrete Research*, Vol. 27, p. 1747, 1997.
7. J. Gonzalez, S. Algaba, and C. Andrade, *Bridge Corrosion Journal*, Vol. 15, p. 135, 1980.
8. A.A. Sagiés, "Corrosion Measurement Techniques for Steel in Concrete," Paper No. 353, Corrosion/93, National Association of Corrosion Engineers, Houston, 1993.
9. A.A. Sagiés, S.C. Kranc, and F.J. Presuel-Moreno, *Applied Modeling For Corrosion Protection Design For Marine Bridge Substructures*, 1997, Final Report, WPI 0510718.
10. H. Liang, "Diffusion Behavior of Calcium Nitrite Corrosion Inhibitor in Concrete," M.S. Thesis, Department of Civil and Environmental Engineering, University of South Florida, Tampa, Florida, May 1999.
11. N.S. Berke, and M.C. Hicks, "Estimating the Life Cycle of Reinforced Concrete Decks and Marine Piles Using Laboratory Diffusion and Corrosion Data," p.207 in *Corrosion Forms and Control for Infrastructure*, ASTM STP 1137, Victor Chacker, Ed., American Society for Testing and Materials, Philadelphia, 1992.
12. L. Bertolini, F. Bolzoni, T. Pastore, and P. Pedferri, "New Experiences on Cathodic Prevention of Reinforced Concrete Structures," *Corrosion of Reinforcement in Concrete Construction*, p. 389, C.L. Page, P.B. Bamforth and J.W. Figg, Eds, The Royal Society of Chemistry, Cambridge, 1996.
13. K. Tuutti, *Corrosion of Steel in Concrete* (ISSN 0346-6906), Swedish Cement and Concrete Research Institute, Stockholm, 1982.
14. P. Bamforth, *Concrete*, p.18, November/December 1994

15. K. Kishitani, I. Fukushi, and H. Shimada, "Promising Concrete Rebars for Construction in Off-shore, Seaside and Desert Environments", *Corrosion of Reinforcement in Concrete Construction*, Chapter 25, p. 419, A.P. Crane, Ed., Society for Chemical Industry, Ellis-Horwood Limited, Chichester, 1983.
16. J. Gonzalez, E. Otero, S. Feliu, and W. Lopez, *Cement and Concrete Research*, Vol. 23, pp. 33-40, 1993.

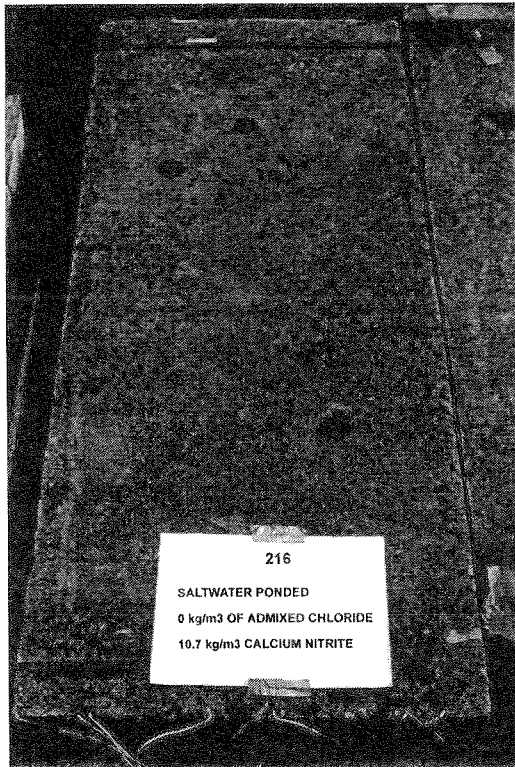
APPENDIX A. PHOTOGRAPHS SHOWING  
SPECIMEN AND TOP STEEL MAT CONDITIONS



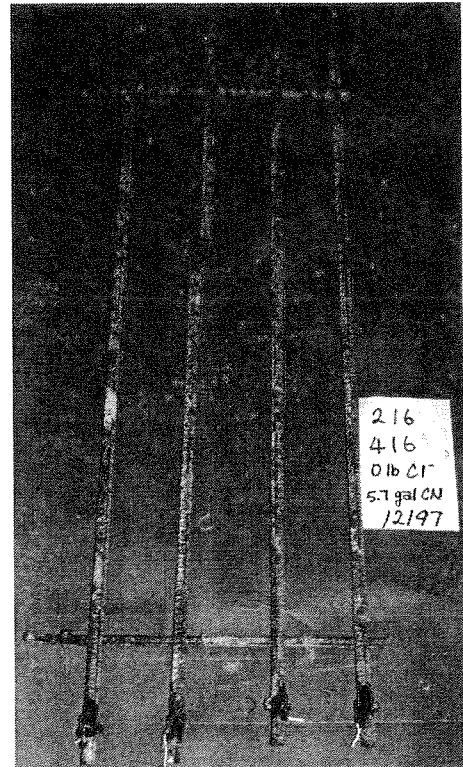
Specimen 211 - 1997



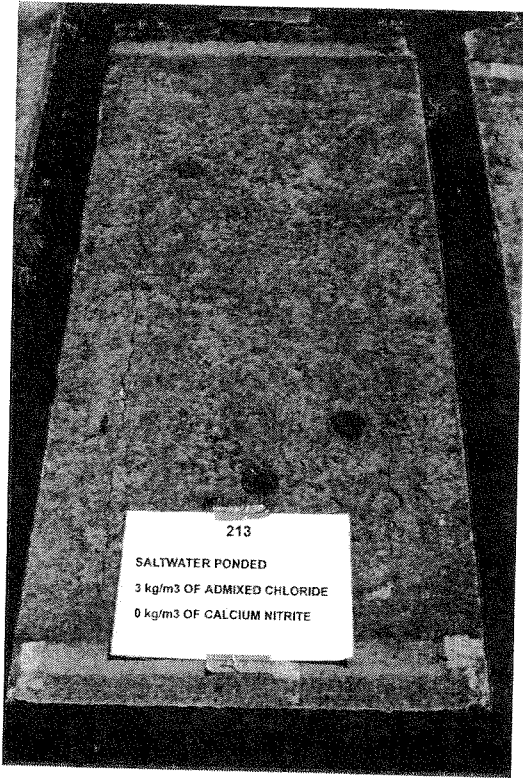
Specimen 211 - Top Steel Mat



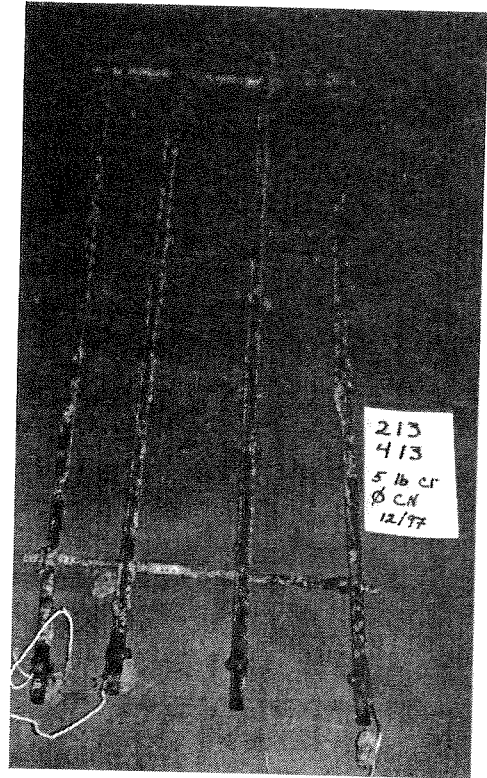
Specimen 216 - 1997



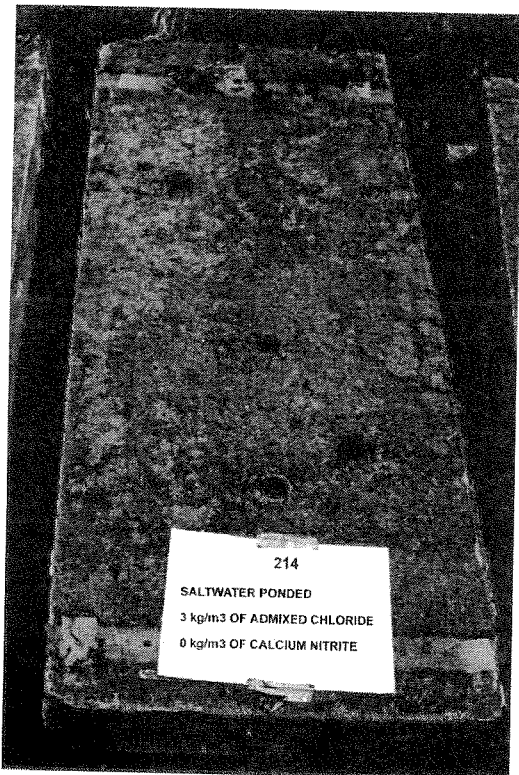
Specimen 216 - Top Steel Mat



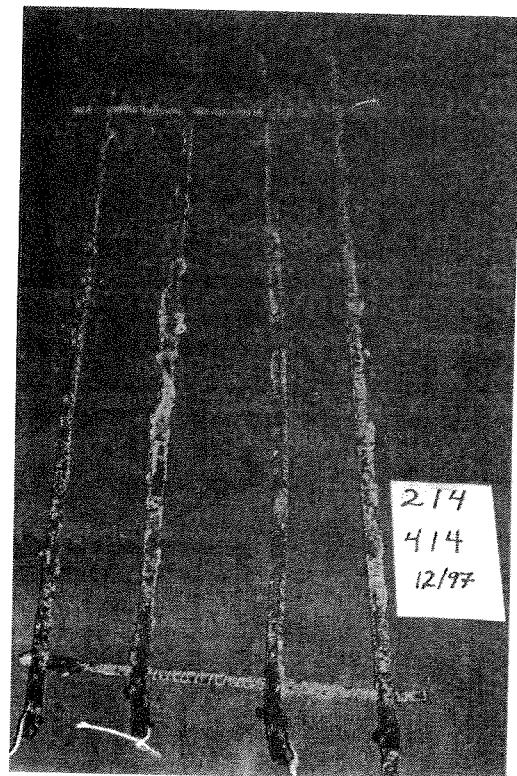
Specimen 213 - 1997



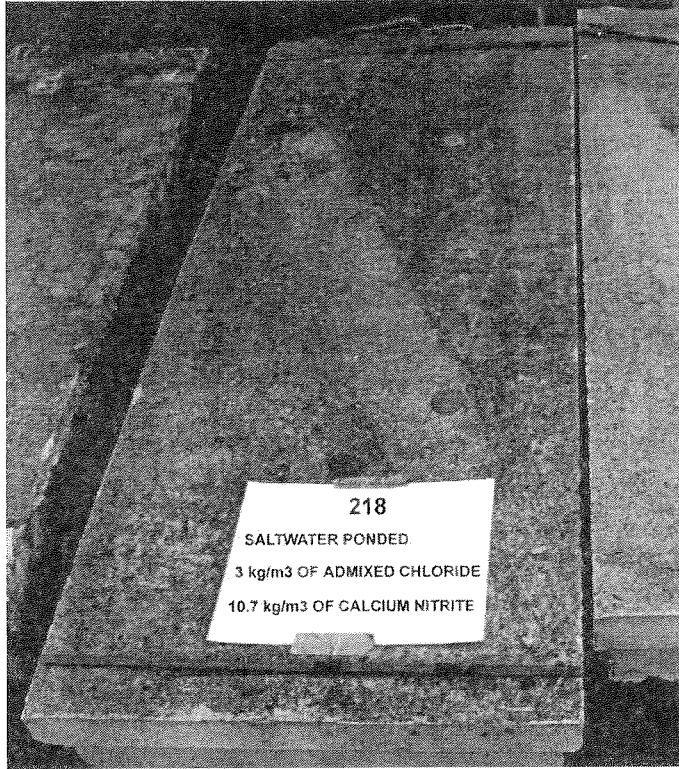
Specimen 213 - Top Steel Mat



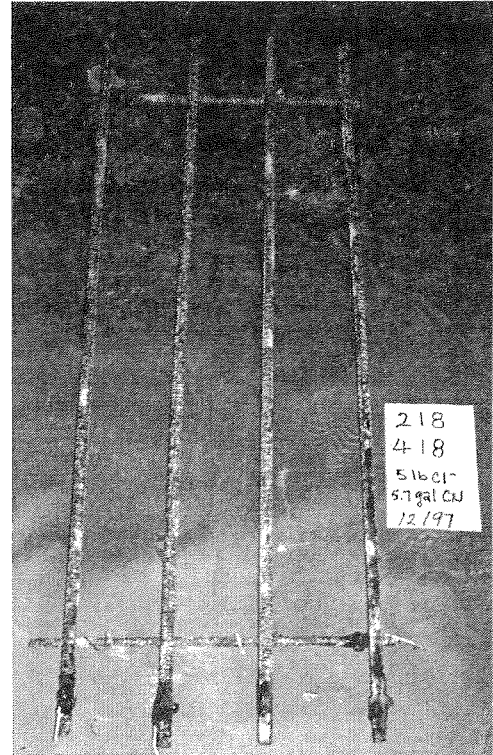
Specimen 214 - 1997



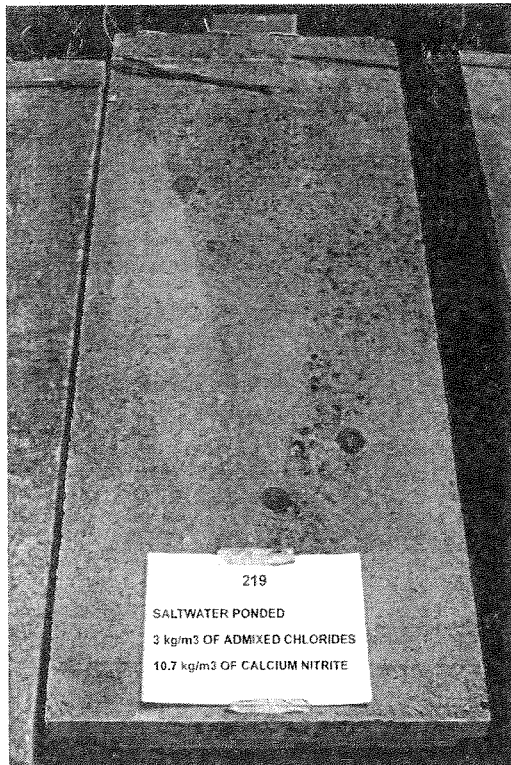
Specimen 214 - Top Steel Mat



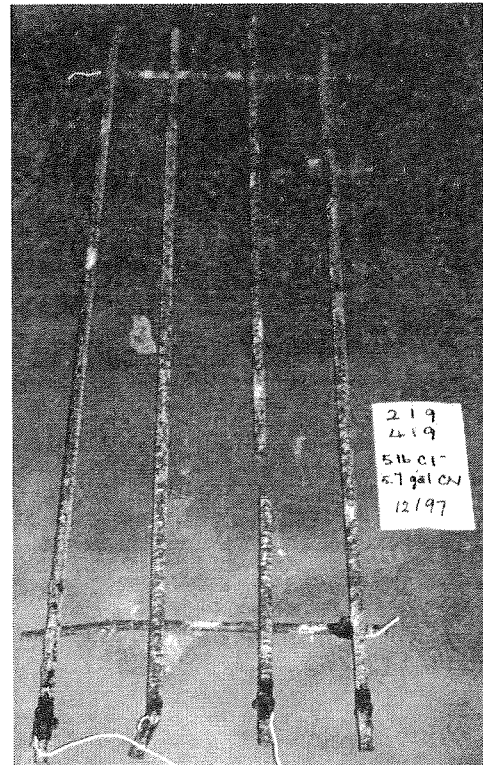
Specimen 218 - 1997



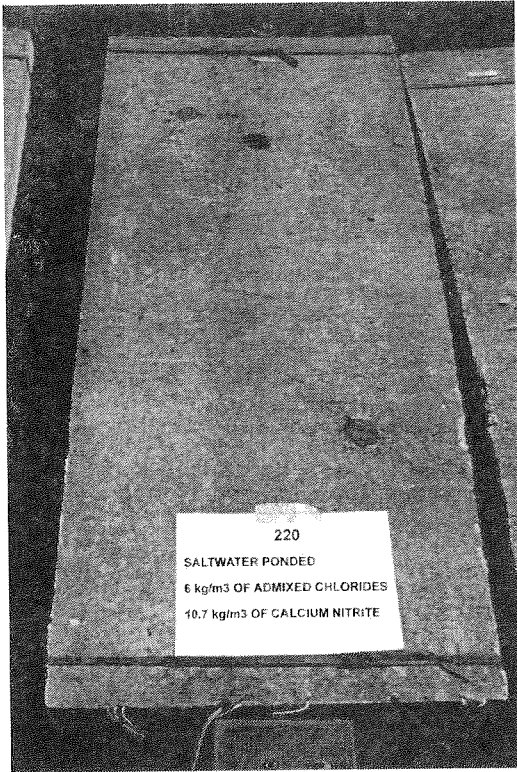
Specimen 218 - Top Steel Mat



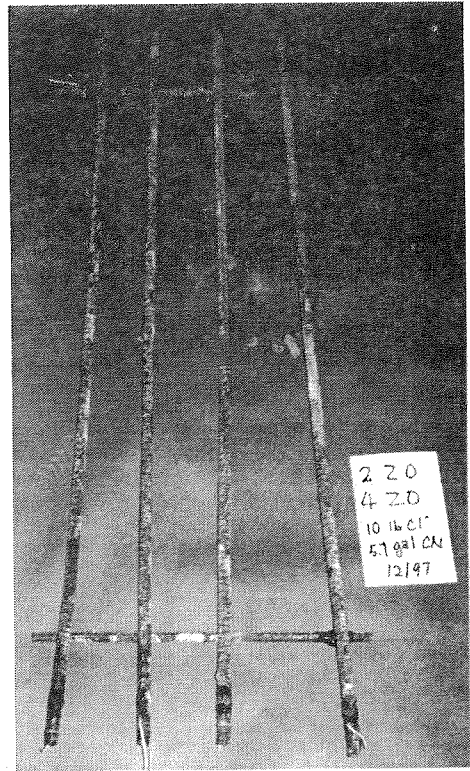
Specimen 219 - 1997



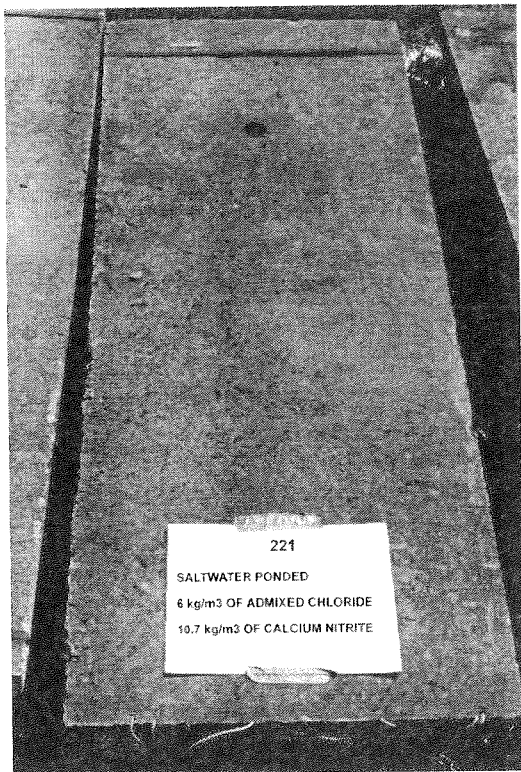
Specimen 219 - Top Steel Mat



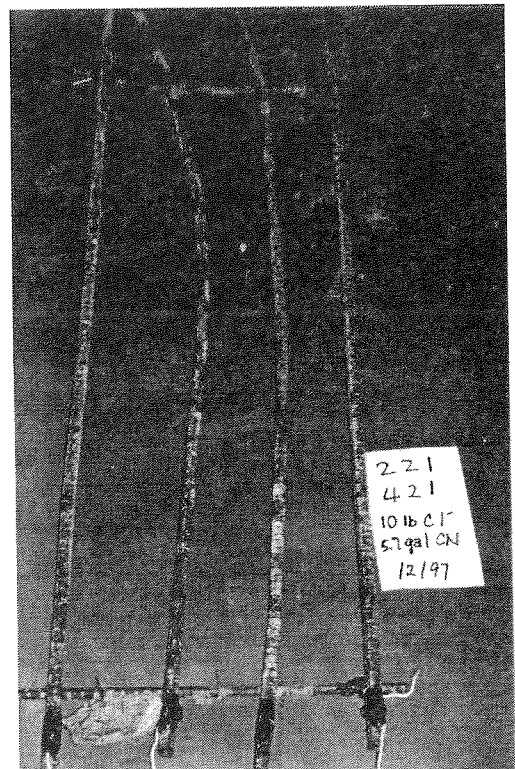
Specimen 220 - 1997



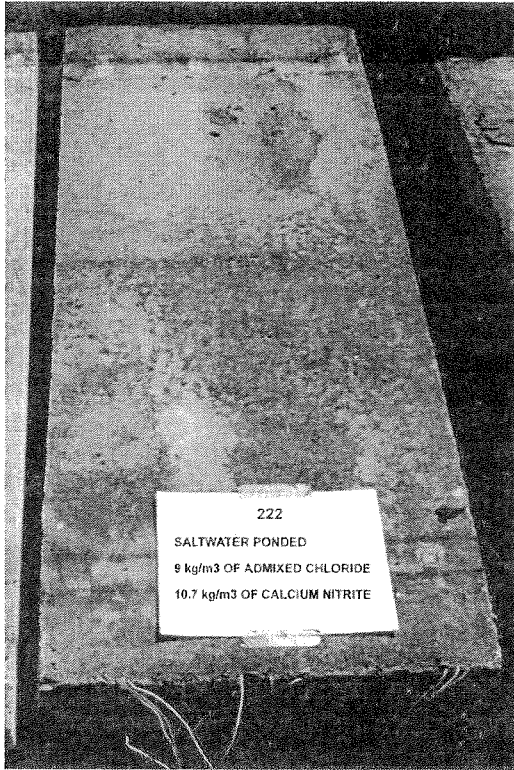
Specimen 220 - Top Steel Mat



Specimen 221 - 1997

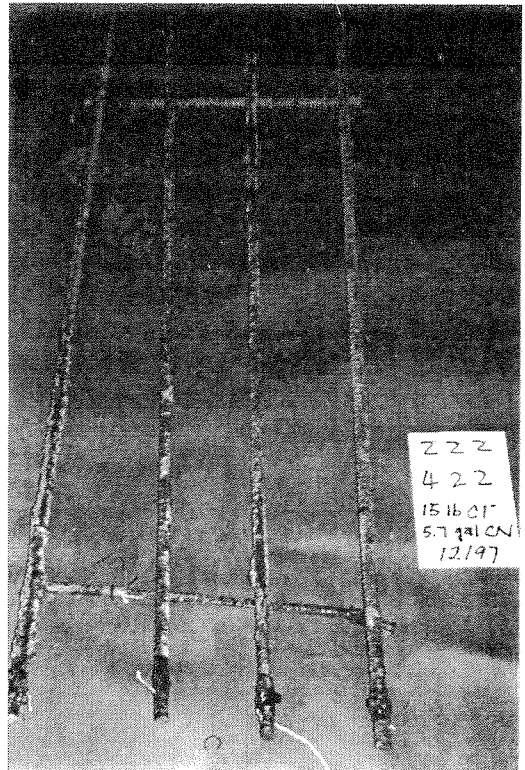


Specimen 221 - Top Steel Mat



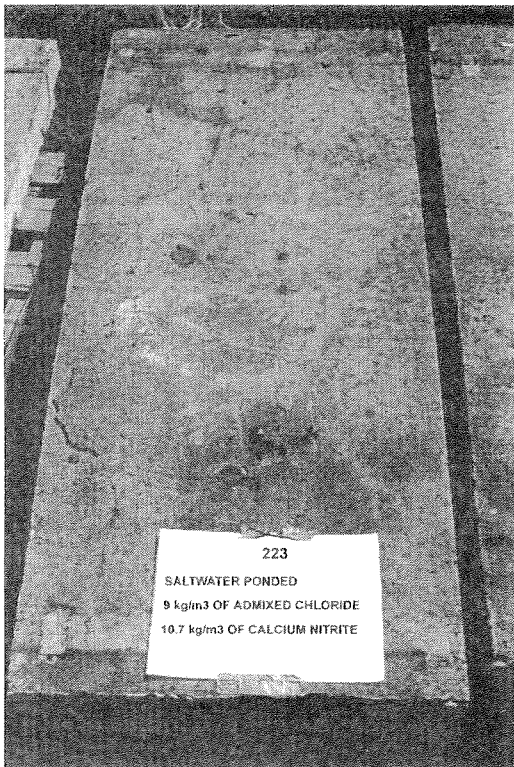
222  
SALTWATER PONDING  
9 kg/m<sup>3</sup> OF ADMIXED CHLORIDE  
10.7 kg/m<sup>3</sup> OF CALCIUM NITRITE

Specimen 222 - 1997



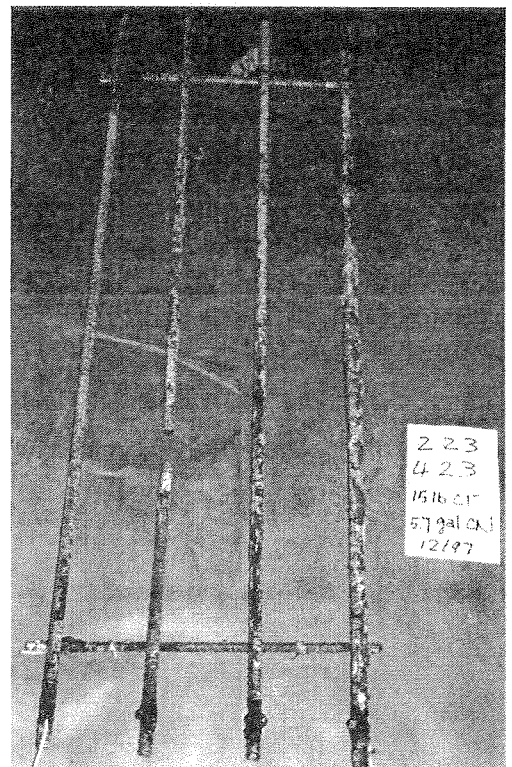
222  
422  
151601  
5.7 gal CN  
12/97

Specimen 222 - Top Steel Mat



223  
SALTWATER PONDING  
9 kg/m<sup>3</sup> OF ADMIXED CHLORIDE  
10.7 kg/m<sup>3</sup> OF CALCIUM NITRITE

Specimen 223 - 1997



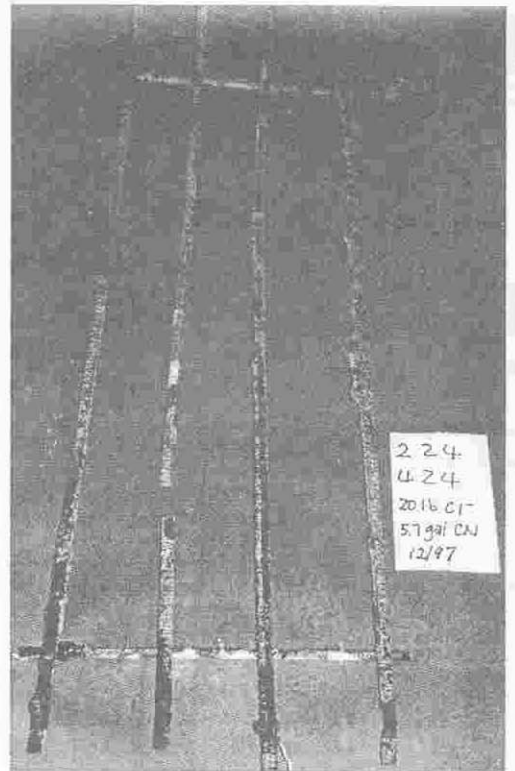
223  
423  
151601  
5.7 gal CN  
12/97

Specimen 223 - Top Steel Mat

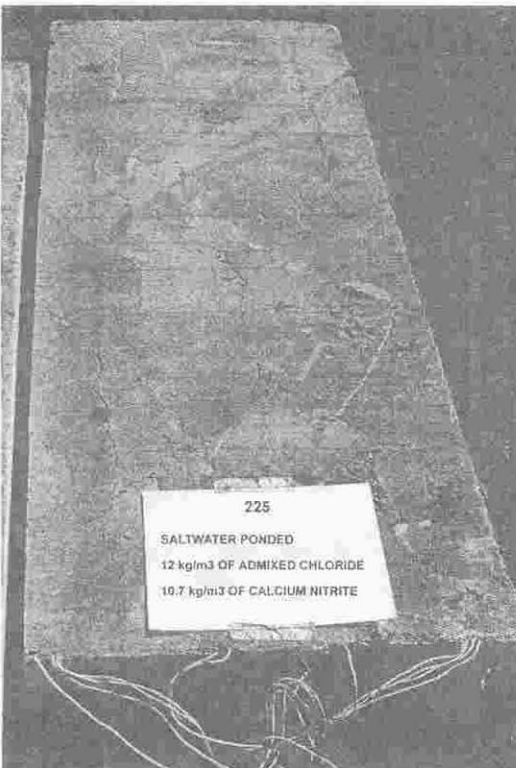




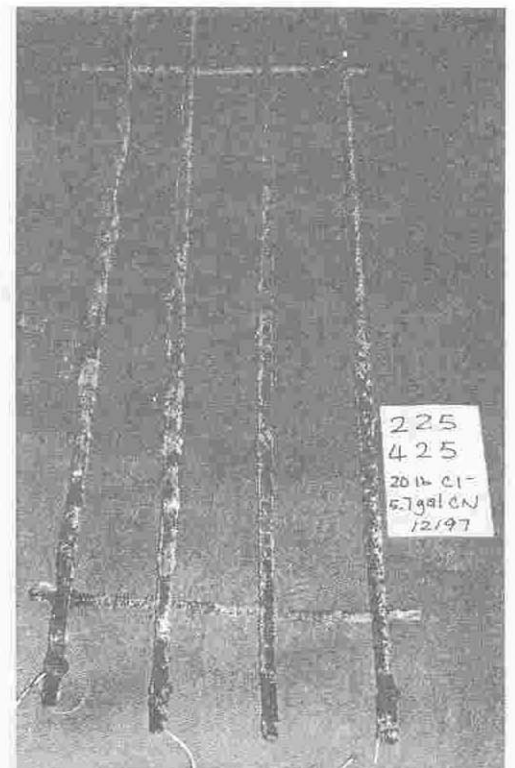
Specimen 224 - 1997



Specimen 224 - Top Steel Mat



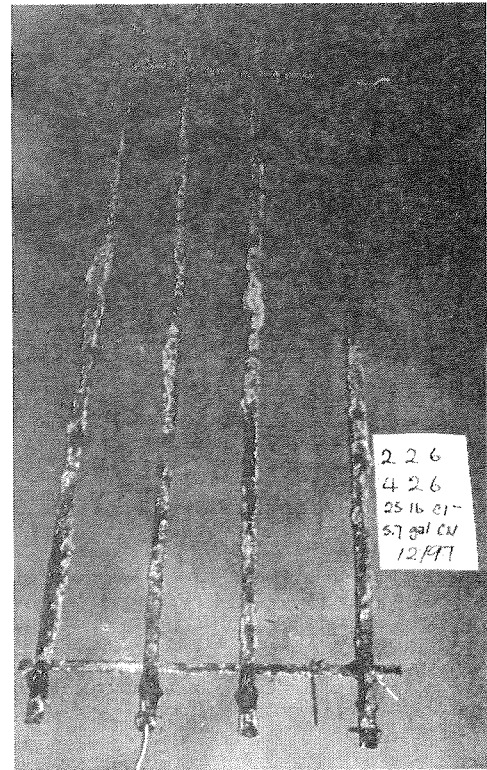
Specimen 225 - 1997



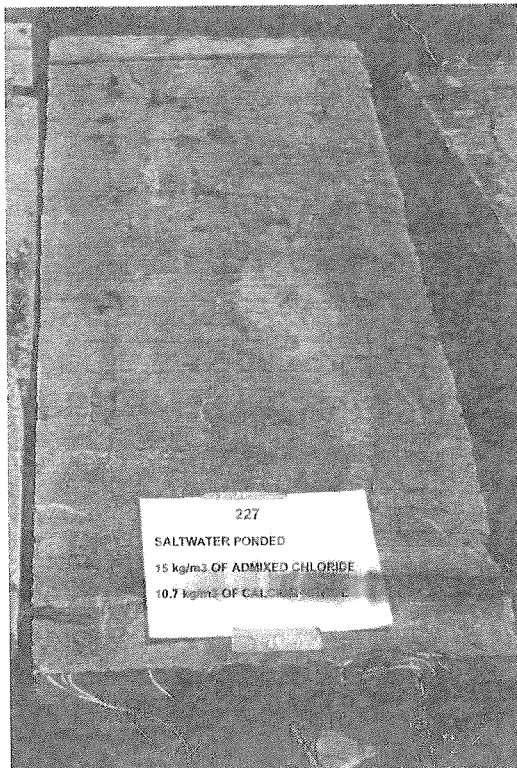
Specimen 225 - Top Steel Mat



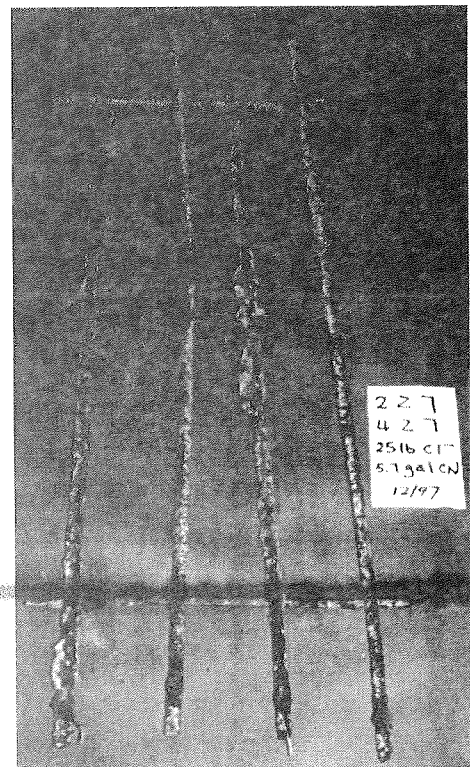
Specimen 226 - 1997



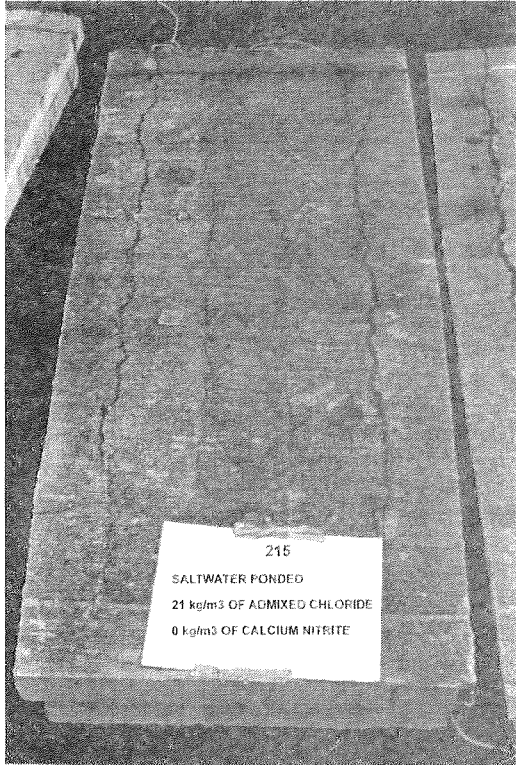
Specimen 226 - Top Steel Mat



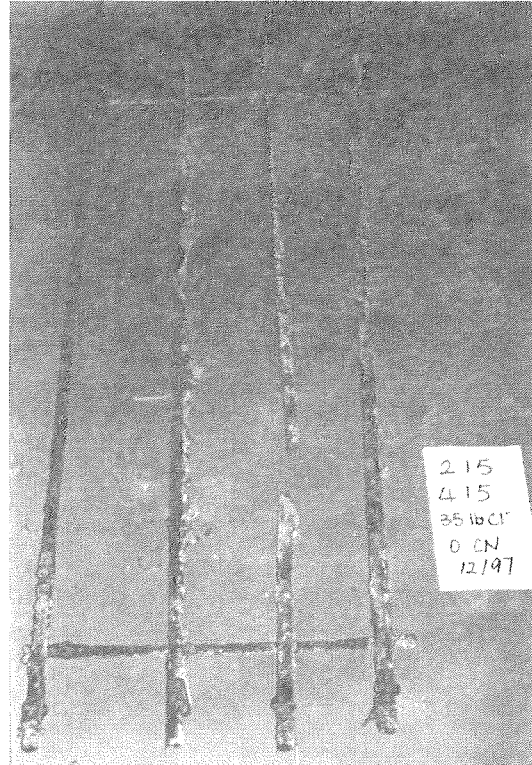
Specimen 227 - 1997



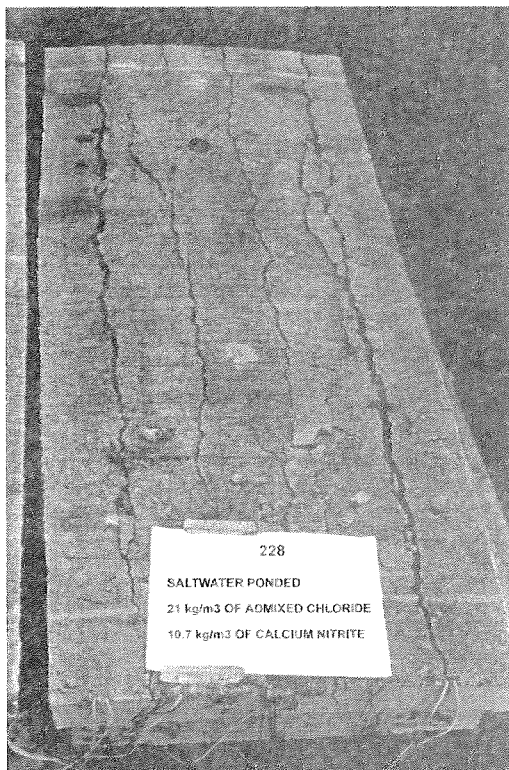
Specimen 227 - Top Steel Mat



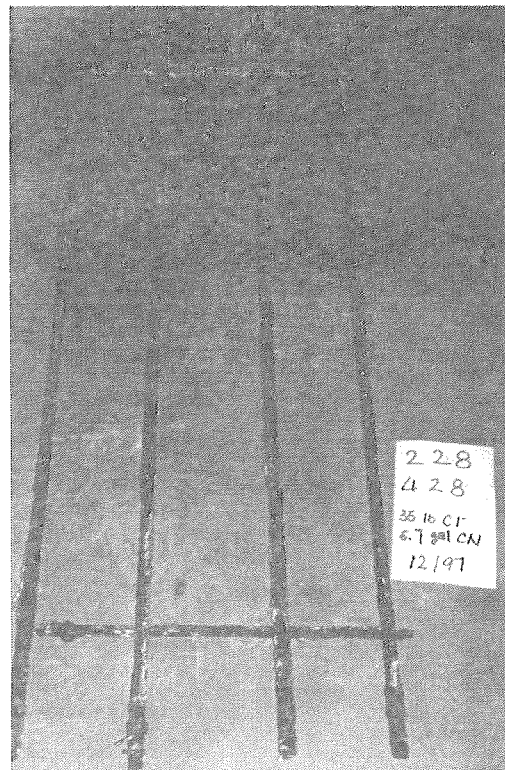
Specimen 215 - 1997



Specimen 215 - Top Steel Mat



Specimen 228 - 1997

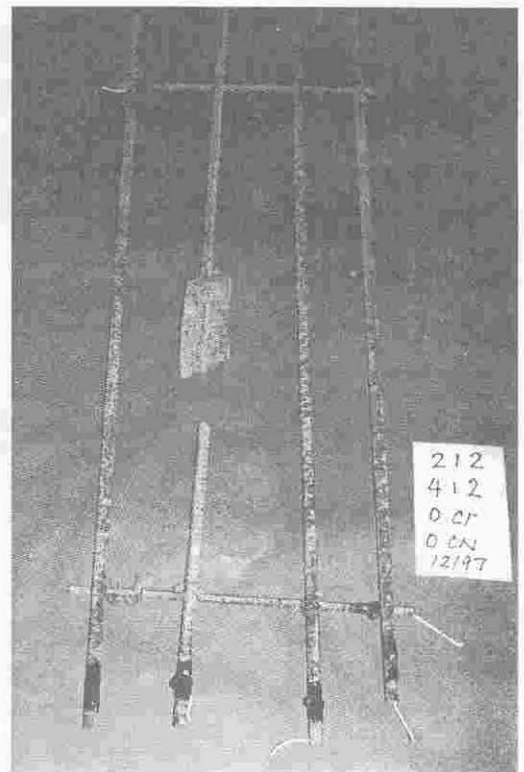


Specimen 228 - Top Steel Mat



212  
NOT POUNDED  
0 kg/m<sup>3</sup> OF ADMIXED CHLORIDE  
0 kg/m<sup>3</sup> OF CALCIUM NITRITE

Specimen 212 - 1997



212  
412  
0.0%  
0.0%  
12/97

Specimen 212 - Top Steel Mat



217  
NOT POUNDED  
0 kg/m<sup>3</sup> OF ADMIXED CHLORIDE  
10.7 kg/m<sup>3</sup> CALCIUM NITRITE

Specimen 217 - 1997



217  
417  
0.16%  
5.7% CN  
12/97

Specimen 217 - Top Steel Mat

## APPENDIX B. ILLUSTRATION OF METHODS USED FOR REPORTING NITRITE CONTENT AND ANALYSIS RESULTS

### *Admixed Nitrite*

Nitrite was admixed as calcium nitrite,  $\text{Ca}(\text{NO}_2)_2$  (molecular weight 132.1), as 2.75 percent of the cement weight. Since the cement factor was  $390.4 \text{ kg/m}^3$ , the calcium nitrite content was  $10.74 \text{ kg/m}^3$ . As the molecular weight of nitrite,  $\text{NO}_2^-$ , is 46.0, the nitrite content was  $7.48 \text{ kg/m}^3$ .

### *Total Nitrite*

Nitrite analyses results were obtained as wt% of the concrete powder tested (the data in Figure 12, obtained from two different laboratories as a procedure test) and were reported in that manner. All calculations were made based on the as-prepared weight of the powdered sample, without further correction for moisture content. Such correction could improve accuracy by a small amount (possibly 2 to 3 percent of the final result), but much of its benefit could be negated by uncertainty in the necessary working assumptions<sup>(1)</sup>; therefore, no moisture correction was made. The nominal unit weight in table 2 was used to convert the wt% into kg of nitrite per unit volume of concrete.

As a nitrite content calculation example, sample 219-4 yielded 0.21 wt% nitrite (figure 12). The corresponding mass per unit volume was  $2,215 \text{ kg/m}^3 \times 0.0021 = 4.61 \text{ kg/m}^3 \text{ NO}_2^-$ . Since the admixed amount was  $7.48 \text{ kg/m}^3$ , the percentage nitrite recovery for that sample was  $100 \times 4.61/7.48 = 61$  percent. That amount is plotted as the fourth data point (counting from the slab top) of the curve for Slab 219 in figure 11.

### *Free Nitrite*

Free nitrite results were obtained by analysis of the concrete cavity water after it was equilibrated with the surrounding pore water. The assumption is made that the cavity water has a composition equal to that of the capillary pore water. A small amount of cavity water was extracted with a syringe, weighed, and diluted in a known amount of distilled water. The  $\text{NO}_2^-$  concentration of the diluted solution was measured spectrophotometrically and the result was converted (using the appropriate dilution factor) to obtain the  $\text{NO}_2^-$  concentration in the cavity water sample. The concentration in the cavity water sample was expressed as mass of  $\text{NO}_2^-$  per mass of cavity water, which was reported in ppm. For example, the sample of cavity water from Slab 219 obtained at 5.1 cm from the top surface had a mass of 18.9 mg and contained 0.187 mg of  $\text{NO}_2^-$ . The free  $\text{NO}_2^-$  concentration was therefore  $10^6 \times 0.187/18.9 = 9917$  ppm.

Expressing the free nitrite in the previous example as a fraction of the total nitrite requires assuming a value for the capillary porosity  $\epsilon$  of the concrete. If  $\epsilon$  is taken to be about 0.1 (a common assumption), then  $1 \text{ m}^3$  of concrete would have  $0.1 \text{ m}^3$  of capillary pore water at 100 percent relative humidity. Assuming for simplicity that the pore water has a density  $\approx 1,000 \text{ kg/m}^3$ , then  $1 \text{ m}^3$  of concrete would contain 100 kg of capillary pore water and, therefore,  $100 \times 9,917/10^6 = 0.99 \text{ kg}$  of free  $\text{NO}_2^-$  for every  $\text{m}^3$  of concrete. Since at the same depth Slab 219 had about 64 percent recovery (figure 11), the total nitrite there was  $\approx 0.64 \times 7.48 = 4.79 \text{ kg/m}^3$ . Therefore, the free nitrite there represented an estimated  $0.99/4.79 \approx 1/5$  of the total nitrite.

**Reference:**

1. H. Liang, N.D. Poor, and A.A. Sagiés, *Enhanced Recovery of Nitrite From Calcium Nitrite-Admixed Hardened Concrete*, to be submitted for publication.